Does deep non-volcanic tremor occur in the central-eastern Mediterranean basin?

Gian Maria Bocchini[1], Patricia Martínez-Garzón[2], Rebecca M. Harrington[3], and Marco Bohnhoff[4]

[1]Faculty of Geosciences, Institute of Geology, Mineralogy, and Geophysics, Ruhr University Bochum
[2]Helmholtz Centre Potsdam GFZ German Research for Geosciences
[3]Ruhr University Bochum
[4]Helmholtz Centre Potsdam GFZ German Research Centre for Geosciences

November 26, 2022

Abstract

Non-volcanic tremor has been observed at the roots of many fault systems around the Pacific rim, including convergent and transform plate boundaries. The extent to which deep tremor signals are prevalent along plate boundaries elsewhere, including the Mediterranean basin, has not yet been documented in detail. A body of evidence suggests that tremor triggered during the surface waves of teleseismic events may commonly occur where ambient tremor during Episodic Tremor and Slip episodes occur, suggesting triggered tremor provides a useful tool to identify regions with ambient tremor. We perform a systematic search of triggered tremor associated with large teleseismic events between 2010 and 2020, at four major fault systems within the central-eastern Mediterranean basin namely the Hellenic and Calabrian subduction zones, and the North Anatolian and Kefalonia transform faults. In addition, we search for ambient tremor during a ˜50-daylong slow slip event in the eastern Sea of Marmara along a secondary branch of the North Anatolian Fault, and two ˜4-month long slow slip events beneath western Peloponnese. We find no unambiguous evidence for deep triggered tremor nor for ambient tremor. The absence of triggered tremor at the Hellenic and Calabrian subduction zones supports the less favorable conditions for tremorgenesis in the presence of old and cold slabs. The absence of tremor along the transform faults may be due to an absence of the conditions commonly promoting tremorgenesis in such settings, including high fluid pressures and low differential stresses between the down-dip limit of the seismogenic layer and the Moho.

Does deep non-volcanic tremor occur in the central-eastern Mediterranean basin?

G. M., Bocchini[1], P., Martínez-Garzón[2], R. M., Harrington[1], and M., Bohnhoff [2, 3]

[1]Faculty of Geosciences, Institute of Geology, Mineralogy, and Geophysics, Ruhr University Bochum, Bochum, Germany

[2]Helmholtz Centre Potsdam GFZ German Research Centre for Geosciences, Section 4.2 Geomechanics and Scientific Drilling, Potsdam, Germany

[3]Institute of Geological Sciences, Free University of Berlin, Berlin, Germany.

†Corresponding author: Gian Maria Bocchini (gian.bocchini@rub.de), Faculty of Geosciences, Institute of Geology, Mineralogy, and Geophysics, Ruhr University Bochum, IA 4/135 Universitätsstr. 150, 44801 Bochum (Germany).

Key Points:

- There is no unambiguous evidence for the occurrence of deep non-volcanic tremor in the central-eastern Mediterranean basin.
- The thermal structure of subduction zones has an important control on deep tremorgenic conditions.
- Very special physical conditions are required for deep tremorgenesis in settings that are not warm subduction zones.

Abstract

Non-volcanic tremor has been observed at the roots of many fault systems around the Pacific rim, including convergent and transform plate boundaries. The extent to which deep tremor signals are prevalent along plate boundaries elsewhere, including the Mediterranean basin, has not yet been documented in detail. A body of evidence suggests that tremor triggered during the surface waves of teleseismic events may commonly occur where ambient tremor during Episodic Tremor and Slip episodes occur, suggesting triggered tremor provides a useful tool to identify regions with ambient tremor. We perform a systematic search of triggered tremor at four major fault systems within the central-eastern Mediterranean basin, namely the Hellenic and Calabrian subduction zones, and the North Anatolian and Kefalonia transform faults, associated with large teleseismic events between 2010 and 2020. In addition, we search for ambient tremor during a ~50-daylong slow slip event in the eastern Sea of Marmara along a secondary branch of the North Anatolian Fault, and two ~4-month long slow slip events beneath western Peloponnese. We find no unambiguous evidence for deep triggered tremor nor for ambient tremor. The absence of triggered tremor at the Hellenic and Calabrian subduction zones supports the less favorable conditions for tremorgenesis in the presence of old and cold slabs. The absence of tremor along the transform faults may be due to an absence of the conditions commonly promoting tremorgenesis in such settings, including high fluid pressures and low differential stresses between the down-dip limit of the seismogenic layer and the Moho.

1 Introduction

The enhancement of geodetic and seismological monitoring systems over the last two decades has led to the discovery of various types of earthquakes, also known as slow earthquakes, with rupture velocities ranging from those of traditional earthquakes with rupture velocities ~2-3 km/s to roughly an order of magnitude faster than plate convergence rates, a few cm/yr (Obara, 2002; Rogers and Dragert, 2003; Obara and Kato, 2016). The range of speeds at which slip is accommodated is usually a function of depth, and may have implications for how plate tectonic loading stress is transferred along dip in major faults, therefore the analysis and interplay of slow and seismogenic earthquakes along fault zones is of particular interest (Schwartz and Rokosky, 2007; Obara and Kato, 2016). Slow earthquakes typically include seismically and geodetically observed events that vary over a range of characteristic time scales

(Obara and Kato, 2016). Seismically observed slow earthquakes include Low Frequency Earthquakes (LFEs) and non-volcanic tremor (hereafter referred to as tremor), with energy often concentrated between frequencies of 2-8 Hz (Obara, 2002), and Very Low Frequency Earthquakes (VLFEs) with energy concentrated between 0.02-0.05 Hz (Ito et al., 2007). Geodetically observed slow earthquakes tend to exhibit slower rupture velocities that do not generate seismic energy, and are subdivided into short-term and long-term Slow Slip Events (SSEs) with durations of days to weeks and months to years, respectively (Wallace et al., 2012; Obara and Kato, 2016). The occurrence of tremor, mostly composed of bursts of LFEs (Shelly et al., 2007), is usually accompanied by short-term SSEs and VLFEs (Obara and Kato, 2016). The coupled manifestation of tremor and short-term SSEs was first discovered in the Cascadia subduction zone (Rogers and Dragert, 2003) and has been termed Episodic Tremor and Slip (ETS). Tremor occurring during ETS episodes is also referred to as spontaneous or ambient tremor.

Several studies locate ETS episodes in subduction zones slightly deeper than the down-dip limit of the seismogenic zone, at depths spanning the intersection of the down-going slab and the upper-plate Moho (Obara, 2002; Wech and Creager, 2008; Brown et al., 2009; Ghosh et al., 2009b; Ide, 2012). ETS episodes along transform plate boundaries, where observed, mostly outline the upper boundary of continental Moho (Nadeau and Dolenc, 2005; Shelly, 2017). Although more widely studied, ETS episodes are not restricted to the down-dip portion of the seismogenic zone (Saffer and Wallace, 2015 and references therein). They have been also documented up-dip or within the seismogenic zone (e.g. Costa Rica, Walter et al., 2011, 2013; NE Japan trench, Nishikawa et al., 2019). In the following, we refer to ETS located below the down-dip limit of the seismogenic zone as deep ETS. The existing ~10-20 km gap between the deep ETS zone and the down-dip limit of the seismogenic layer is often filled by long-term SSEs (Obara, 2011; Husker et al., 2012; Wech, 2016; Gao and Wang, 2017) and does not appear to be strongly correlated to tremor and VLFEs (Husker et al., 2012; Obara, 2011).

Although the underlining physical mechanisms remain enigmatic, it is commonly accepted that slow earthquakes may straddle a transitional physical state between conditions favoring stick-slip behavior and conditions favoring stable sliding (Audet and Kim, 2016). It also appears that fault thermal structure affects the depth distribution and occurrence of slow earthquakes (Ide, 2012; Yabe et al., 2014; Gao and Wang, 2017) due to the primary temperature control on the brittle-plastic transition (Scholz, 1998). Numerical models with thermo-petrologically controlled rheology suggest the occurrence of the brittle-plastic transition at depths shallower than the upper-plate Moho as *conditio sine qua non* for slow earthquake occurrence in subduction zones (Gao and Wang, 2017). In fact, tremor has been primarily observed at young, warm subduction zones (Obara, 2002; Wech and Creager, 2008; Brown et al., 2009; Ide, 2012) where the brittle-plastic transition and peak dehydration reactions occur at shallower depths than in cold subduction zones (Peacock and Wang, 1999). However, the thermal structure of faults can be controlled by factors other than age (Yabe et al., 2014; Gao and Wang, 2017). For example, the often observed patchy nature of spatial deep tremor distribution (Ghosh et al., 2009b; Ide, 2012), indicates that tremor is also affected by other mechanisms such as pore fluid pressure (Kodaira et al., 2004; Audet et al., 2009), rock frictional properties (Houston, 2015), fault geometrical complexities (Romanet et al., 2018), sea floor irregularities and properties of overriding plate (Nishikawa et al., 2019). Seismological investigations often reveal the presence of near-lithostatic pore fluid pressures (e.g. high Vp/Vs ratios) in regions where tremor does occur (Kodaira et al., 2004; Audet et al., 2009; Audet and Kim, 2016;). Hence, the presence of high fluid pressure that reduces the effective stresses and the frictional strength along the fault is the mechanism most commonly invoked to control deep tremor generation within a transitional physical state (Kodaira et al., 2004; Audet and Kim, 2016; Gao and Wang, 2017). Similar conditions are proposed to control tremor generation up-dip of the seismogenic zone in subduction zones (Saffer and Wallace, 2015). Hence, potentially tremorgenic conditions could exist along many faults and possibly at different depths. However, to date, the description of favorable and non-tremorgenic conditions is practically limited to the observations along the Pacific rim and does not extend to fault systems where diverse physical and geological conditions may coexist such as in the Mediterranean basin.

In fault zones where ambient tremor is observed during ETS episodes, it is also commonly triggered during the passing of surface waves from teleseismic events (hereafter referred to as triggered tremor) (Fig. 1; e.g. Gomberg et al., 2008; Miyazawa et al., 2008; Miyazawa and Brodsky, 2008; Peng and Chao, 2008; Ghosh et al., 2009a; Fry et al., 2011; Chao et al., 2012a, 2012b, 2013). As triggered tremor typically has larger amplitudes than ambient tremor (Rubinstein et al., 2007), a systematic search for triggered tremor provides a useful tool to identify regions that might also experience (undocumented) ambient tremor.

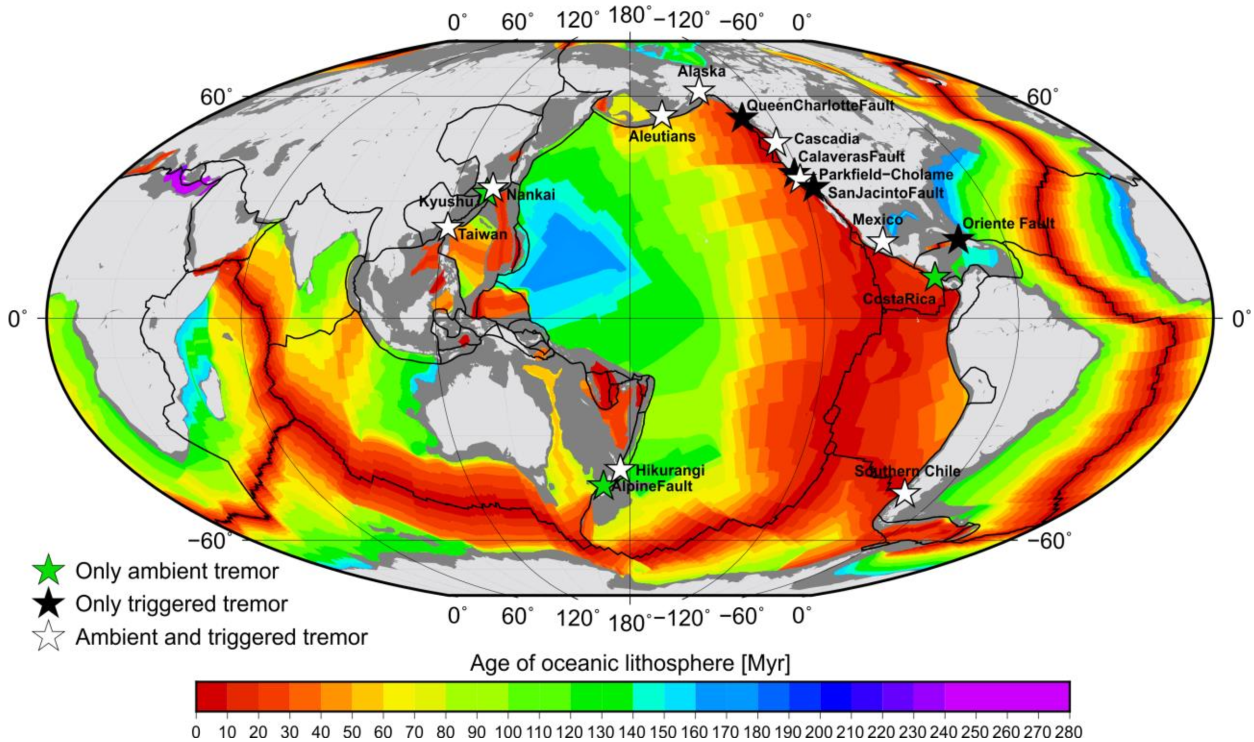

Figure 1. *Global distribution of well-documented (observed at a minimum of three stations) sources of triggered and ambient tremor, which is confined primarily to the Pacific rim (Nadeau and Dolenc, 2005; Brown et al., 2009, 2013; Peng et al., 2009; Kim et al., 2011; Chao et al., 2012a, 2013; Ide, 2012; Wech et al., 2012; Aiken et al., 2013; Sun et al., 2015; Nishikawa et al., 2019). Note the inverse correlation between the occurrence of tremor and the age of the subducting oceanic lithosphere, which is colored according to age (Müller et al., 2008).*

Teleseismically induced Peak Ground Velocities (PGV) as low as 0.01-0.03 cm/s, corresponding to dynamic stresses of about 1-3 kPa, are also capable of triggering tremor (Miyazawa and Brodsky, 2008; Peng et al., 2009; Chao et al., 2012a). Tremor triggering thresholds appear to be variable from region to region (Peng and Gomberg, 2010) and may depend on several factors including instrumentation differences and background tremor activity (Chao et al., 2012a). Furthermore, in some locations, tidally induced stress changes on the order of ~1 kPa seem to be capable of triggering tremor (Thomas et al., 2009; Houston, 2015; van der Elst et al, 2017). Despite the growing observations of ambient and triggered tremor, one of the most striking features of all well-documented cases (i.e. visible at least at three seismic stations), is that they are confined to transform and convergent plate boundaries, or fault systems, along the Pacific rim (Fig. 1). To date, the Oriente Fault near Guantanamo Bay (Cuba) represents the only exception with observed triggered tremor during two teleseismic events (Peng et al., 2013). Whether the absence (or infrequent occurrence) of deep tremor outside of the Pacific rim is due

to a sampling bias or to non-favorable physical conditions is still poorly understood. The dearth of studies reporting null results, i.e. an absence of tectonic tremor (Yang and Peng, 2013; Bockholt et al., 2014; Pfohl et al., 2015) make it hard to address such a question.
In this work, we perform a systematic search of triggered tremor within the central-eastern Mediterranean basin (Fig. 2). The region is generally well instrumented due to its intense seismic activity, and therein subduction zones exhibit different physical (e.g. old/cold subducting lithosphere and slower converge rates) and depositional conditions (e.g. thicker and wider accretionary wedges) compared to the Pacific rim. Moreover, for instance, its major transform faults, namely the Kefalonia and North Anatolian Fault, have formed more recently and have accumulated smaller relative displacement (Şengör et al., 2005; van Hinsbergen et al., 2006) than the Alpine and San Andreas Faults (Dickinson and Wernicke, 1997; Norris and Cooper, 2001), where tremor has been documented (Fig. 1). Hence, it is well suited to further explore necessary and inhibiting physical conditions for tremor occurrence. In the specific, we focus on four major active fault systems, namely the Hellenic and Calabrian subduction zones, and the Kefalonia and Marmara section of the North Anatolian transform faults (Fig. 2), where no unambiguous example of ambient and triggered tremor has been reported to date. In all analyzed regions, sufficient seismic station coverage was available over the past 10 years which is sufficient to detect triggered tremor, should it have occurred. Although the main focus of this study is triggered tremor, we also investigate the occurrence of ambient tremor during a SSE in the eastern Marmara Sea, along the North Anatolian Fault, and two SSEs beneath Peloponnese, in the western segment of the Hellenic Subduction Zone.

We limit our analysis to subduction zones and transform faults because they host the multitude of observed triggered and ambient deep tremor worldwide (Fig. 1). In Section 2 we provide a tectonic overview of the study regions, followed by a description of the datasets and methods in Section 3. We report the results in Section 4 and discuss, together with the implications of our study, the similarities and differences with other fault systems in Section 5. Conclusive remarks of the study are in Section 6.

2 Plate Boundaries in the central-eastern Mediterranean

The current tectonic setting of the Mediterranean area arose from a complex interaction between the long-lasting but comparatively slow convergence of the African and Eurasian plates

(Faccenna et al., 2014). Deformation concentrates along irregular and diffuse boundaries between fragments of continental and oceanic lithosphere moving independently from the overall convergent motion (Fig. 2) (Faccenna et al., 2014). Historical and instrumental seismicity, defined by frequent low-to-moderate and occasionally large (M>7) magnitude earthquakes (Guidoboni and Comastri, 2005), concentrates along the plate and microplate boundaries (Fig. 2). Compared to the western portion, the central-eastern Mediterranean basin releases larger seismic moment and displays larger strain rates (Martínez-Garzón et al., 2020). The oldest *in situ* oceanic lithosphere on Earth (>220-230 Ma) is currently subducting at the Hellenic and Calabrian Arcs (Granot, 2016; Müller et al., 2008; Speranza et al., 2012). These very narrow and arcuate subduction arcs (Faccenna et al., 2014), and the thick and wide accretionary prisms (Clift and Vannucchi, 2004) make the Mediterranean basin a unique region worldwide (Fig. 1-2).

In this region, the occurrence of slow earthquakes is still poorly investigated, and, to date, there is no unambiguous evidence of deep tectonic tremor in the Mediterranean basin. The Hellenic (Fig. 2c) and Calabrian (Fig. 2b) subduction zones, as well as the Kefalonia (Fig. 2a) and North Anatolian transform faults (Fig. 2d), share similar faulting styles with those of fault systems where deep tremor has been documented and therefore represent potential candidates for hosting deep tremor in the central-eastern Mediterranean.

Although all formed in the broad tectonic context of Africa-Eurasia convergence, the four fault systems developed at different times and present distinct seismotectonic settings (e.g. kinematics, seismic moment release, age). In the following subsections (2.1-2.4) we delineate the main seismotectonic properties of the regions selected for the search for tremor. We focus on the description of seismotectonic and geological aspects that are relevant to deep tremorgenic conditions.

2.1 The Kefalonia Transform Fault

The Kefalonia Transform Fault (Fig. 2a) marks the western termination of the Hellenic Subduction Zone (Louvari et al., 1999; Pérouse et al., 2012; Bocchini et al., 2018). It started to form in the late Miocene-early Pliocene and has accumulated most of its ~60 km of total displacement over the last ~4-5 Ma (van Hinsbergen et al., 2006). The fault accommodates ~2 cm/yr of differential convergence between oceanic subduction and continental collision taking place to the north and south, respectively (Pérouse et al., 2012). It is composed primarily of two active segments, namely the Kefalonia and the Lefkada segments (Fig. 2a) and exhibits pure right-lateral or transpressional slip motion (Louvari et al., 1999). The fault frequently generates M>6 earthquakes (Papazachos and Papazachou, 2003; Papadimitriou et al., 2017). The distribution of earthquakes suggests a seismogenic layer extending between 3 and 16 km (Papadimitriou et al., 2017), with a crustal Moho at ~28 km (Sodoudi et al., 2006). To date there is no documented evidence of slow earthquakes along the Kefalonia Transform Fault.

2.2 The Calabrian Subduction Zone

The Calabrian Subduction Zone (Fig. 2b) forms a narrow, arcuate subduction interface in southern Italy. The subduction of ~220-230 Ma old oceanic crust (Speranza et al., 2012) began ~80 Ma ago (Faccenna et al., 2001), and currently continues along a ~150 km wide sector between the Isthmus of Catanzaro to the north and the Strait of Messina to the south (Fig. 2b) (Maesano et al., 2017). The incoming plate has a 5-6 km thick layer of sedimentary cover forming a large accretionary prism (de Voogd et al., 1992). The subduction convergence rate is < 5 mm/yr (Pérouse et al., 2012), and has documented intraslab seismicity down to ~450-500 km (Selvaggi and Chiarabba, 1995), as well as a depletion of shallow interplate seismicity offshore in the Ionian Sea. The very low interplate seismicity and the low strain rates in the forearc (~10-20 nanostrain/yr) led some authors to consider the subduction as inactive (e.g. Pérouse et al., 2012). However, a recent study interprets unambiguous geodetic signals consistent with elastic strain accumulation at the megathrust being released episodically seismically and/or more likely through aseismic slip transients (Carafa et al., 2018). The interpretation also reconciles with the large historical earthquake data in Calabria (Carafa et al., 2018), and could suggest the occurrence of slow earthquakes.

2.3 The Hellenic Subduction Zone

The Hellenic Subduction Zone (Fig. 2) defines an approximately 1000 km long arcuate interface bounded to west by the Kefalonia Transform Fault and to the east, beneath south-western Turkey, by a tear in the slab (Bocchini et al., 2018). Oceanic lithosphere of age >220-230 Ma to the west (Speranza et al., 2012), and likely >300 Ma to the east (Granot, 2016) is currently subducting at a rate of ~35-40 mm/yr (McClusky et al., 2000). The down-going plate is overlaid by a wide sediment layer forming the Mediterranean Ridge Accretionary Prism which spans roughly up to 10-12 km thickness and is ~250-300 km long (e.g. Bohnhoff et al., 2001; Kopf et al., 2003). Nubian-Aegea convergence generates intense seismicity, even for M > 4(Fig. 2), and earthquakes as large as M~8 as reported in historical catalogues (Papazachos and Papazachou, 2003). Seismological and geodetic studies suggest that more than 70-80% of the relative plate motion occurs asesimically (Becker and Meier, 2010; Vernant et al., 2014; Saltogianni et al., 2020). Very recently, Mouslopoulou et al. (2020) reported two SSEs beneath the western coast of Peloponnese south of Zakynthos (Fig. 1Sb). Both SSEs were preceded by ~2 months of plate motion acceleration. The first geodetic transient started on 09/24/2014 and terminated on 03/20/2015, with the actual SSE starting on 11/29/2014. The second started on 05/14/2018 and terminated on 10/25/2018, with the actual SSE starting on 07/10/2018. Both SSEs are suggested to occur between 20 and 40 km depth along the plate interface. To date, no evidence of tectonic tremor is reported along the active margin between the down-going and overriding plates.

Crete represents a horst structure in the central Hellenic forearc (Fig 2c) currently undergoing fast uplift and extension (Meier et al., 2007). Subduction south of Crete started about 20–15 Ma, when the plate boundary stepped back to the southern edge of an accreted microcontinent, building most of the continental crust of present Crete (Thomson et al. 1998). The megathrust south of Crete, exhibits intense microseismicity that abruptly terminates at ~40 km depth below the southern coastline of the island (Meier et al., 2004), where the upper-plate crustal thickness is ~30-35 km (Bohnhoff et al., 2001; Meier et al., 2007).

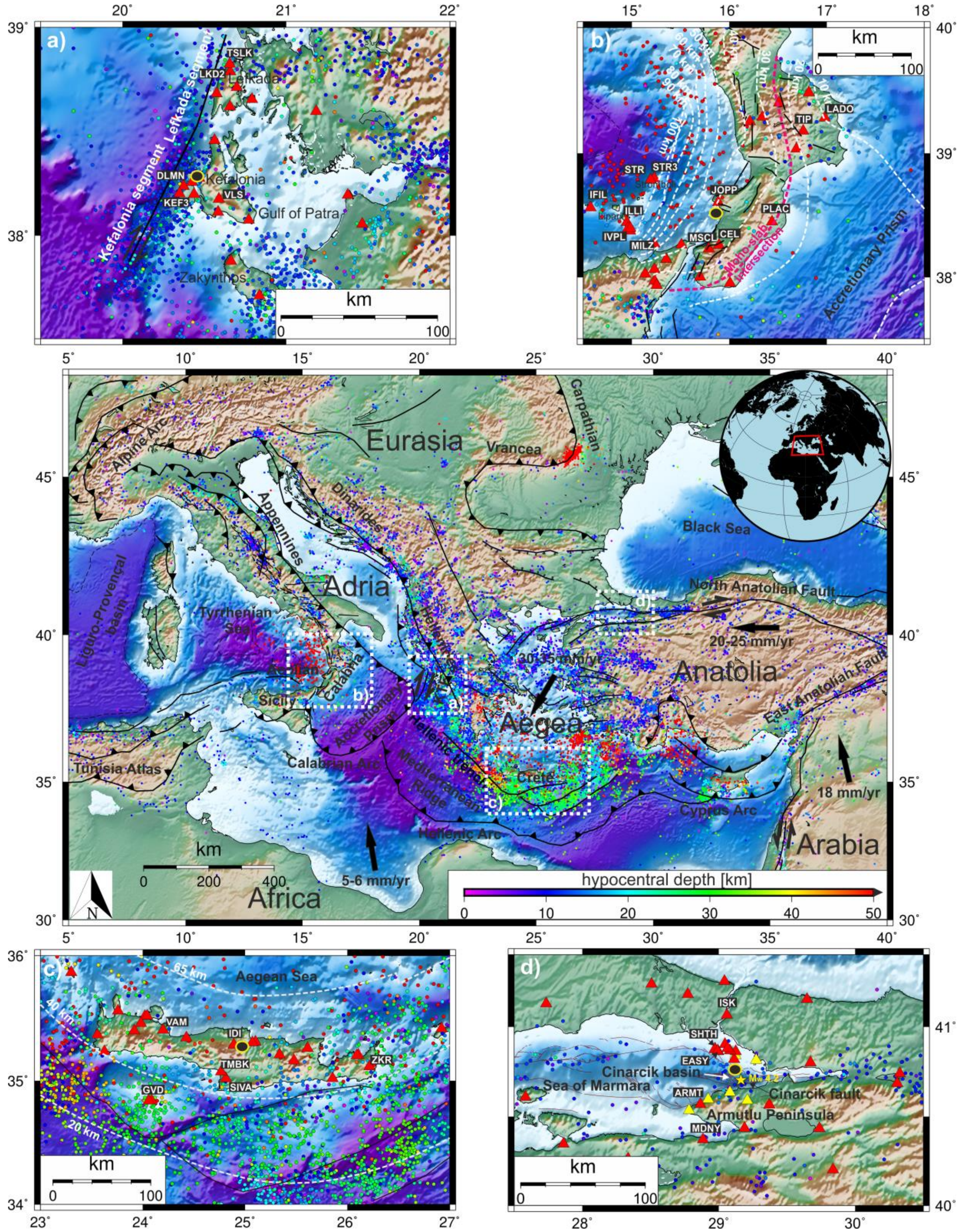

Figure 2. *Main panel: Central and eastern Mediterranean region. Main tectonic elements (black lines) from Faccenna et al., (2014). Black arrows indicate the relative plate-microplate motion with respect to stable Eurasia (McClusky et al., 2000). Earthquake hypocentral locations (dots) are color coded according to depth, saturated to 50 km. We plot all earthquakes with M>4*

documented by the International Seismological Centre (ISC) between 1964-2010 (ISC, 2020). Dotted white boxes in the main panel indicate the four study regions: a) Kefalonia Transform Fault, b) Calabrian Subduction Zone; c) Hellenic Subduction Zone, Crete; d) North Anatolian Fault, eastern Marmara Sea. Red triangles indicate the maximum number of available seismic stations (not necessarily available in all investigated periods), where station names used in Fig. 4 are shown in white. Yellow triangles in panel c indicate borehole stations. Dashed lines in panels b-c represent the top of the slab isodepths from Maesano et al., (2017) and Bocchini et al., (2018), respectively. Dashed magenta line in panel b indicates the location of the intersection with the overriding plate Moho. Yellow star in panel (d) indicates the epicentral location of the Mw 4.2 Yalova earthquake on June 25, 2016. Black circles with yellow edges indicate the location where initial Peak Ground Velocity values were estimated (see Section 3). Bathymetry is from Ryan et al., (2009).

2.4 The North Anatolian Fault.

The North Anatolian Fault is a 1200-km-long right-lateral transform fault forming the boundary between the Eurasian Plate and the Anatolian microplate with relative displacement of ~20-25 mm/yr (Fig. 2) (McClusky et al., 2000). It started to form 12-13 Ma ago during the late phase of Arabia-Eurasia collision that accumulated a maximum displacement of ~85-90 km decreasing from east to west (Bohnhoff et al., 2016). The North Anatolian Fault is well-known for its intense seismicity and frequent M>7 earthquakes (Bohnhoff et al., 2016), such as the earthquake sequence in the 20th century that ruptured all but the Sea of Marmara segments (Stein et al., 1997). The Sea of Marmara region (Fig. 2d) representing the western portion of the North Anatolian Fault is in a transtensional state and represents a pull-apart basin within two major branches of the North Anatolian Fault that are ~100 km apart (Armijo et al., 2002). It formed as part of a NS-extensional regime related to the fast rollback of the Hellenic Subduction Zone with the strike-slip regime being active since ~2.5 Ma (Şengör et al., 2005; Le Pichón et al., 2016). The northern part of the Sea of Marmara is characterized by the presence of three deep basins separated by bathymetric highs, from east to west: the Çınarcık, Central, and Tekirdag basins (Armijo et al., 2002). The Çınarcık basin is bounded to the south by the Çınarcık fault and formed ~1.7-2.0 Ma accommodating ~2 km of N-S extension and ~18 km of right-lateral deformation (Carton et al., 2007). Precise hypocentral solutions suggest a seismogenic layer extending down to 10-15 km in the eastern Sea of Marmara (Wollin et al., 2018) while the Moho is found at 26-41 km depth (Zor et al., 2006; Jenkins et al., 2020).

The analysis of recent high temporal resolution geodetic data revealed the existence of temporal fluctuations of the creep rate with detection of accelerating bursts of shallow (i.e. 0-5 km) creep events (i.e. SSEs) along the segments of the North Anatolian Fault that ruptured during the 1999 Izmit earthquake (Aslan et al., 2019) and the 1944 Ismetpasa earthquake (Rousset et al., 2016). On 25 June 2016, a ~50-daylong SSE was recorded along the Çınarcık fault below the eastern Sea of Marmara (Martínez-Garzón et al., 2019). The authors obtain the best fit between calculated and observed signal, assuming the source location to be near to the M_w 4.2 Yalova earthquake (Malin et al., 2018) occurred during the onset of the SSE (Fig. 2d). The strain release during the SSE was equivalent to a M_w 5.8 at the depth of 9 km (Martínez-Garzón et al., 2019). However, the depth remains poorly constrained due to its recording at a single station.

A previous study found no evidence for triggered tremor and no unambiguous evidence for ambient tremor on the central segment of the North Anatolian Fault near Ismetpasa (Pfohl et al., 2015), while here we focus on the recently densely instrumented eastern Sea of Marmara (Fig. 2d).

3 Data and Methods

In the description that follows, we restrict the analysis in the Hellenic Subduction Zone to the segment south of Crete due to the higher open-access seismic station density and data quality relative to adjacent segments. For the North Anatolian Fault, we focus on the eastern Sea of Marmara because of the waveform data from dense local network deployments that are available. In addition, we search for ambient tremor in the eastern Sea of Marmara, eventually related to the ~50-daylong SSE and the M_w 4.2 event along the Çınarcık fault (Fig. 2d) on June 25, 2016 (Martínez-Garzón et al., 2019), and during the two ~6-month long aseismic transients, and related SSEs, beneath Peloponnese, along the western segment of the Hellenic Subduction Zone (Mouslopoulou et al., 2020).

As a first criteria to search for triggered deep tremor, we identify prospective triggering teleseismic earthquakes by selecting all events with Mw ≥ 6.5, hypocentral depths ≤ 50 km, and epicentral distances ≥ 800 km that generated a theoretical PGV larger than 0.01 cm/s within each study region. We restrict our analysis to large and shallow potential triggering mainshocks because they are most effective in generating large surface waves at teleseismic distances, and hence have the greatest potential of triggering tremor. We calculate theoretical PGV values at a point in the middle of each study region (Fig. 2a-d) using a ground motion empirical relationship (Aki and Richards, 2002; Lay and Wallace, 1995):

$$Ms = \log A20 + 1.66 \log \Delta + 2.0 \quad (1)$$

$$PGV \approx 2\pi\, A20/T \quad (2)$$

where Ms is the surface wave magnitude, A20 is the amplitude (in microns) of the Airy phase (surface wave with a 20 s period), Δ is the source-receiver (epicentral) distance, and T is the surface wave period (20 s). We assume M_s=M_w as first approximation. We download all mainshock candidate waveforms from the European Integrated Data Archive (EIDA, http://www.orfeus-eu.org/data/eida/). In addition to publicly available data, we use data from dense local deployments, namely the PIRES network (GFZ Potsdam BU-Kandilli, 2006) and the GONAF borehole network (Bohnhoff et al., 2017) to search for triggered tremor in the eastern Sea of Marmara.

As a second criteria for culling the list of candidate mainshocks, we calculate the observed PGV_{obs} value as the average value between the three components from all the available broad-band stations within each region (Fig. 2a-d), and reject the events which average PGV_{obs} < 0.01 cm/s (Fig. 3a-d). We retain a total of 16 candidates for the Hellenic and Calabrian subduction zones and for the Kefalonia Transform Fault and 18 events for the North Anatolian Fault (Fig. 3 a-d, Table S1). A complete list of analyzed events is reported in Table S1. Nearly all selected mainshocks are either strike-slip or reverse faulting earthquakes (Fig. 3a-d). They cover a wide range of back azimuthal directions, with a limited gap to the south (Fig. 3e-h).

To manually search for cases of triggered tremor, we visually inspect waveforms surrounding the time interval predicted for the passage of surface waves in each study region. We calculate theoretical surface wave arrivals using the TauP package and the iasp91 velocity model (Kennett and Engdahl, 1991) in Obspy (https://docs.obspy.org/packages/obspy.taup.html), and search temporal windows starting when a phase travelling at 4.4 km/s (approximate Love wave arrival) reaches the station and terminates with the predicted arrival of a Rayleigh phase travelling at 2.0 km/s. The time window choice ensures that Love and Rayleigh waves with the highest triggering potential and amplitudes are included in the analysis. We rotate horizontal components to transverse and radial directions to visually confirm the correct arrival time of Love and Rayleigh waves, respectively. Following a well-established procedure, we search for non-impulsive, coherent signals, applying either a 2-8 Hz bandpass filter or a 5 Hz highpass filter to remove the low-frequency teleseismic signal (i.e. primary and secondary arrivals) and preserve tremor signals in the frequency band where it is commonly observed to be most energetic. We require any prospective triggered tremor signal to be recorded by at least three seismic stations in order to be sure that the signal is local and of tectonic origin.

In addition to visual inspection, we also employ an envelope cross-correlation (Ide, 2012, 2010) to detect ambient tremor during the SSE in the eastern Sea of Marmara during an extended time period from (06/02/2016 to 07/30/2016) encompassing the SSE (Martínez-Garzón et al., 2019) and the two SSEs, in 2014-2015 and in 2018, along the western segment of the Hellenic Subduction Zone (Mouslopoulou et al., 2020). The procedure entails creating daily envelopes of signals filtered between 2 and 8 Hz and cross-correlating horizontal channels at stations located <100 km apart. An event is detected when a minimum cross-correlation value (0.5-0.7) is exceeded at a minimum number of channels (5-8). A more detailed description of the method is available at Ide (2010; 2012) and it is also provided in the supplement along with details on the station configuration (Text 1S). In Figure 2S, we report an example of ambient tremor detected using the envelope cross-correlation method employed in this study (Fig. 2S). We detect several tremor signals near the Parkfield-Cholame segment of the San Andreas Fault, where tremor is widely documented (Nadeau and Dolenc, 2005; Shelly, 2017), using the same settings as for the eastern Sea of Marmara (Fig. 2S). We are aware of the limitations of the detection method in the absence of the dense network coverage (Fig. 1S) that is needed to detect low amplitude correlated signals, particularly in the presence of intense background seismic activity that could mask possible tremor signals. However, although search of triggered tremor remains the focus of the paper, the occurrence of SSEs that could be associated with the occurrence of LFE/tremor activity warrants an additional search for ambient tremor.

343 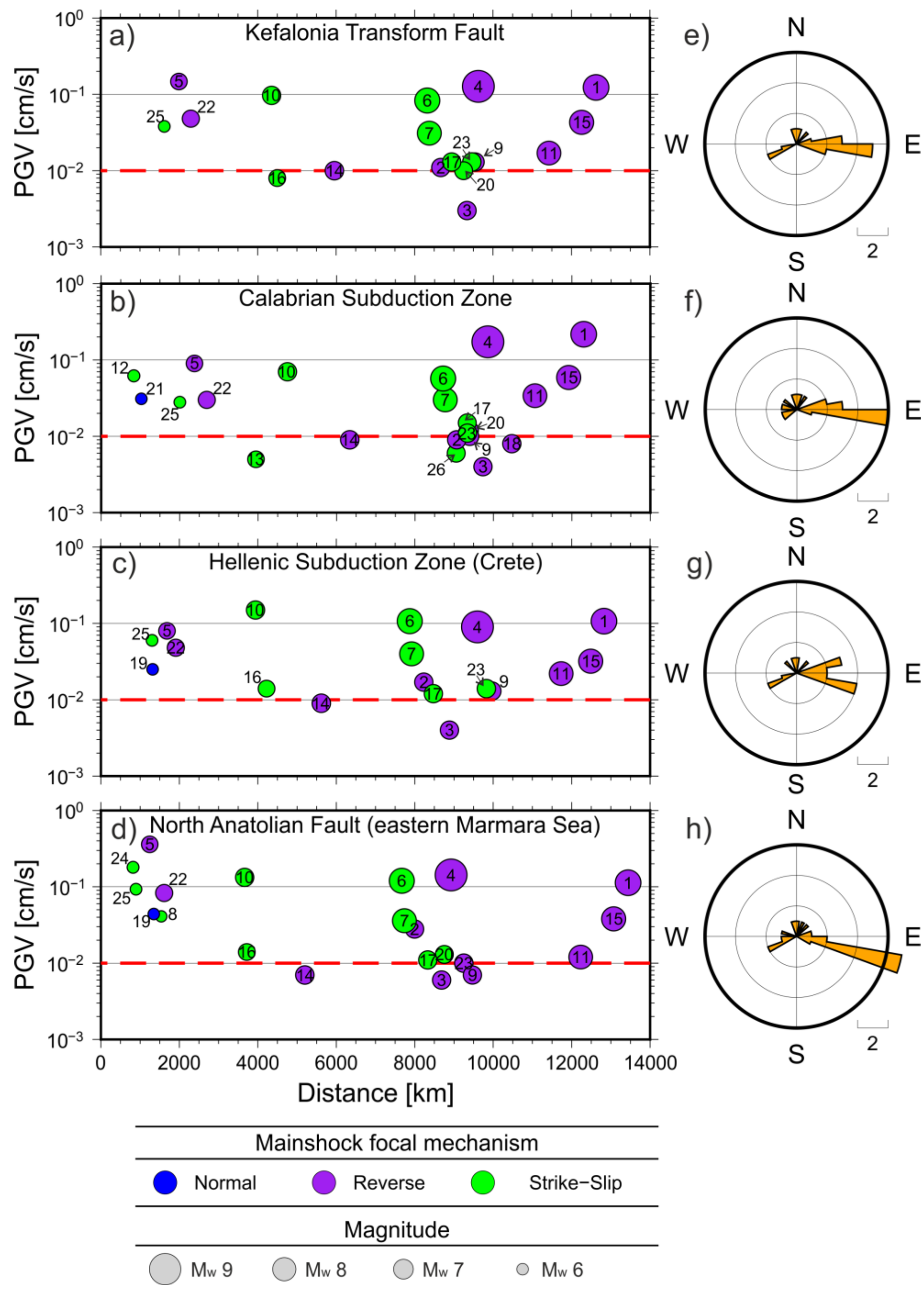

Figure 3. *List of candidate mainshocks around which the search for triggered deep tremor is centered (a-d). (a-d) Symbol sizes correspond to magnitude, while color code corresponds to focal mechanism type. Dotted red lines indicate lower threshold of 0.01 cm/s Peak Ground Velocities (PGV) considered for mainshock candidates in this study. Observed PGV (PGV_{obs}) is calculated as the average value (unfiltered traces) among the three components of all the available broad-band stations within each region. (e-h) Back azimuths of candidate mainshocks producing PGV_{obs} > 0.01 cm/s. Numbers are event IDs and associated events are reported in Table S1.*

4 Results

The manual inspection of waveforms during the passage of surface waves from events in Table S1 at seismic stations along four major fault systems within the central-eastern Mediterranean basin reveals no unambiguous case of triggered tremor at any of the study areas, nor for ambient tremor during the documented SSEs. We first document the observations for triggered tremor (4.1), followed by ambient tremor below (4.2).

4.1 Triggered tremor

We find no unambiguous evidence for triggered tremor beneath Crete, along the Hellenic subduction zone, beneath Calabria at the Calabrian subduction zone, at the Kefalonia Transform Fault, and in the eastern Sea of Marmara, along the North Anatolian Fault, during the time period from 2010 to 2020 considered here. Although the minimum number of three stations may be a strict criterion relative to previous studies, we also do not observe coherent tremor-like signals if reducing the minimum number of required stations to two. In Figure 4, we show high frequency waveforms at a sample of stations during surface wave ground shaking of mainshock candidates inducing some of the largest PGV_{obs} within each region as a representative example of the lack of tremor energy.

We do observe potentially triggered low frequency signals at stations located along the Aeolian Arc, the volcanic arc of the Calabrian Subduction Zone (Fig. 2b). Two of the most striking signals are observed at station ILLI on Lipari Island (Fig. 3S) and at stations ISTR and IST3 on Stromboli (Fig. 4S). However, despite the good correlation between PGV_{obs} and low frequency signal occurrence, we cannot consider them as triggered signals. First, neither case fulfills the criterion of tremor-like signals exhibiting signal coherency at minimum three stations. In addition, careful inspection of the waveforms from one day before to one day after the mainshock reveals that the signal detected at station ILLI (Fig. 3S) is likely noise, due to the highly regular and repetitive nature of the candidate tremor signal (starting at ~6 am and ending at ~5 pm) in the frequency band of interest (2-8 Hz and higher). The signal we observe at stations ISTR and IST3 on Stromboli (Fig. 4S) is very likely a LFE of volcanic origin, however, we note that we also observe several LFEs events both before and after the ground shaking induced by the teleseismic event. Moreover, the slab interface at the closest stations to where the tremor-like signal is observed is located at ~100 km depth beneath the volcanic Arc (Maesano et al., 2017). A seismic signal originating at 100 km depth would not support a seismic source originating from the ETS zone, which is expected at shallower depths where the slab intersects the overriding plate, corresponding to ~25 km depth at the observed location (Fig. 2b).

The seismic stations on Crete exhibit evidence for a single tectonic tremor candidate during the M_w 8.3 Illapel (Chile) earthquake (ID 15 in Fig. 3, Tab. 1S). However, although visible at 3-4 stations (Fig. 5S) the signal is observed before the arrival of surface waves, when PGV_{obs} is smaller than 0.01 cm/s, suggesting an ambient, rather than triggered origin. We explore the possibility that the detected signal (Fig. 5S) could represent ambient tremor by running match filter detection in EQcorrscan (Chamberlain et al., 2018). We used 6-8s second-long signal time windows, filtered between 2-8 Hz, to correlate with continuous data in one-day time windows before and after the tremor-like signal occurrence. Observations of ambient tremor in other fault zones rarely document isolated tremor events, but more commonly clustered, prolonged activity. The matched filter detection yielded no additional detections of similar low frequency signals, in spite of testing a range of settings.

At seismic stations along the Kefalonia Transform Fault we do not observe any tremor like signal. We observe, as in the other regions, possible dynamically triggered local earthquakes (see example in Fig. 4a), however, we will dedicate further investigation of remote dynamic earthquake triggering to a follow-up study, as the purpose of this work is to investigate the occurrence of tectonic tremor. Unfortunately, for the Kefalonia Transform Fault we have only 2-3 stations available during the passage of surface waves of the M_w 8.8 2010 Maule and the M_w 9.1 2011 Tohoku earthquakes, the largest events occurred between 2010 and 2020.

Finally, we do not observe tremor activity during the passage of surface waves in the eastern Sea of Marmara. The latter represents the better instrumented region in our study. Observed correlated signals are either associated to local earthquakes or to instrument/cultural noise.

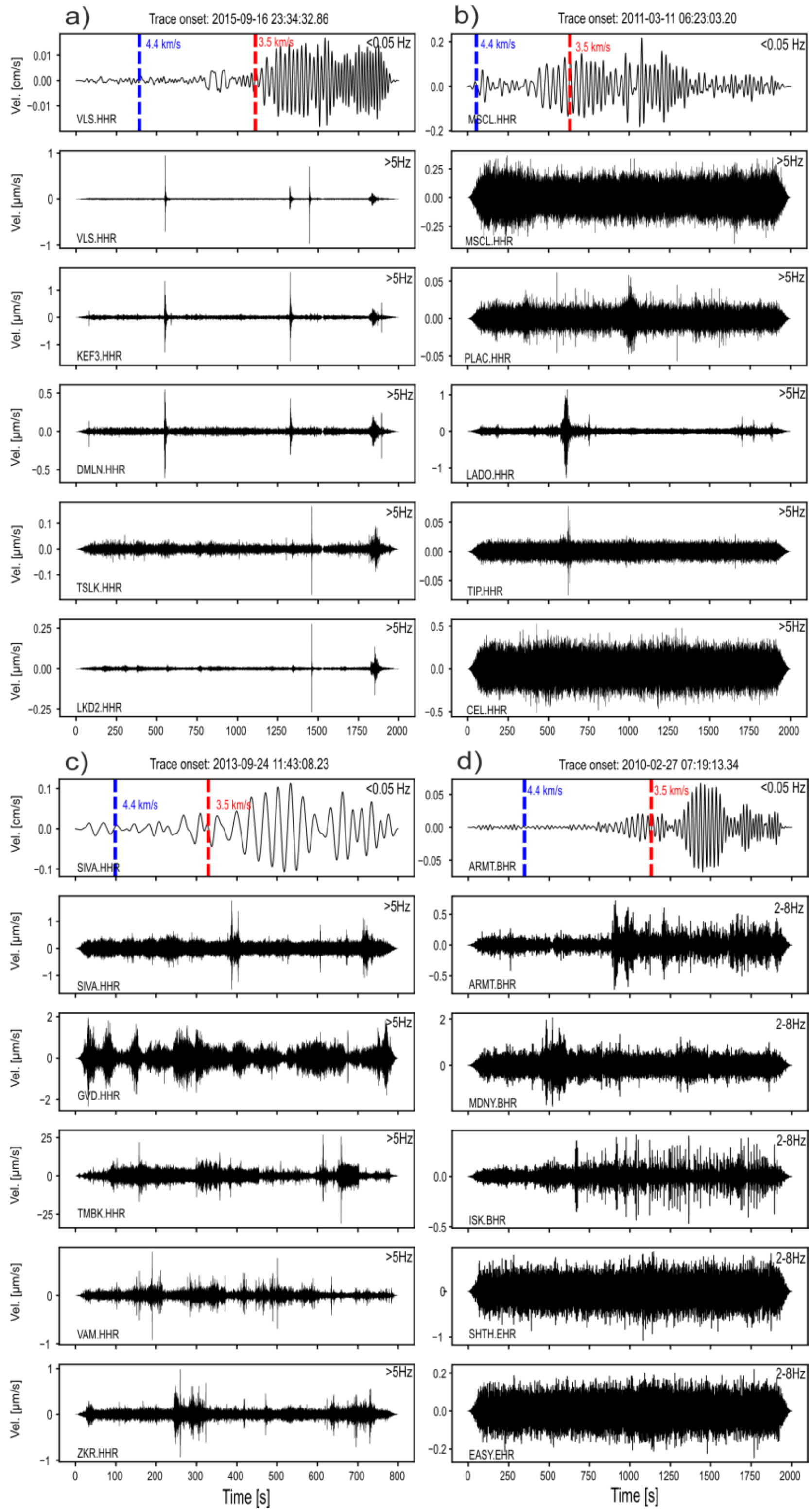

Figure 4. *Example of waveforms exhibiting a lack of evidence for triggered tremor at the a) Kefalonia Transform Fault, during the M_w 8.3 Illapel (Chile) earthquake (ID 15 in Fig.3 and Tab. 1S); b) Calabrian Subduction Zone, during the M_w 9.1 Tohoku (Japan) earthquake (ID 3 in Fig.3 and Tab. 1S); c) Hellenic Subduction Zone (Crete), during the M_w 7.8 Pakistan earthquake*

(ID 10 in Fig.3 and Tab. 1S); d) Eastern Marmara Sea (North Anatolian Fault), during the M_w 8.8 Maule (Chile) earthquake (ID 1 in Fig.3 and Tab. 1S). The candidate triggering earthquakes are among those generating the largest recorded PGV_{obs} locally (Fig. 3). The onset time of the signals in each region is indicated on top of each panel. Three clear local earthquakes (one between 500 and 750 sec and two between 1250 and 1500 sec) are visible at the Kefalonia Transform Fault (a), and a more distant earthquake is visible between 1750 and 2000 sec. In other regions, only uncorrelated noise is visible except for stations LADO and TIP at the Calabrian Subduction Zone (b) where a local signal is visible between 500 and 750 sec. The dashed red and blue lines in the topmost panels indicate the estimated arrival time of phases travelling at 4.4 and 3.5 km/s, respectively, used as preliminary arrival time of Love and Rayleigh waves. The location of seismic stations used herein is shown in Fig. 2a-d.

4.2 Ambient tremor

We find no unambiguous examples of LFE/tremor activity accompanying the SSEs in the eastern Marmara Sea and beneath western Peloponnese. Such result, although possibly affected by the limitations described before in Section 3, are consistent with the absence of triggered tremor along the investigated plate margins. As suggested by examples elsewhere in the world, triggered tremor tends to occur in regions where also ambient tremor occurs (Fig. 1).

In addition to local earthquakes with energetic signals in the frequency band both higher than 10 Hz and in the 2-8 Hz frequency band, we detect signals with dominant frequencies in the tectonic tremor frequency band (2-8 Hz, Fig. 5). However, other factors suggest that the signals as shown in Figure 5, are not tectonic tremor. The signal in Figure 5a has, at the closest station, a duration > 15 sec and a frequency content <10 Hz. However, at stations exhibiting a higher Signal-to-Noise-Ratio (e.g. DRO Fig. 5a), the same signal more closely resembles a local earthquake rather than tremor. We also detect signals (S-waves) from more distant earthquakes that could be misinterpreted as an LFE if one restricted observation of such phases to stations located near SSEs sources where tremor activity would be expected (Fig 5b). For example, the signal shown in Figure 5b, exhibits low frequency energy at stations on the Armutlu Peninsula (e.g. ARMT, KURT, YLV), however, at stations located to the west of the Marmara Sea (e.g. KRBG, RKY) the typical character of an earthquake appears clear. Because of the occurrence of several examples as those reported in Figure 5, we visually check all the detections. At the Hellenic Subduction Zone, due to the longer cumulative duration of the two geodetic transients (~1 year), we checked all detected signals with duration longer than 15 seconds (through a preliminary investigation we observed that signals shorter than 15 seconds were mostly local earthquakes and in very few cases noise).

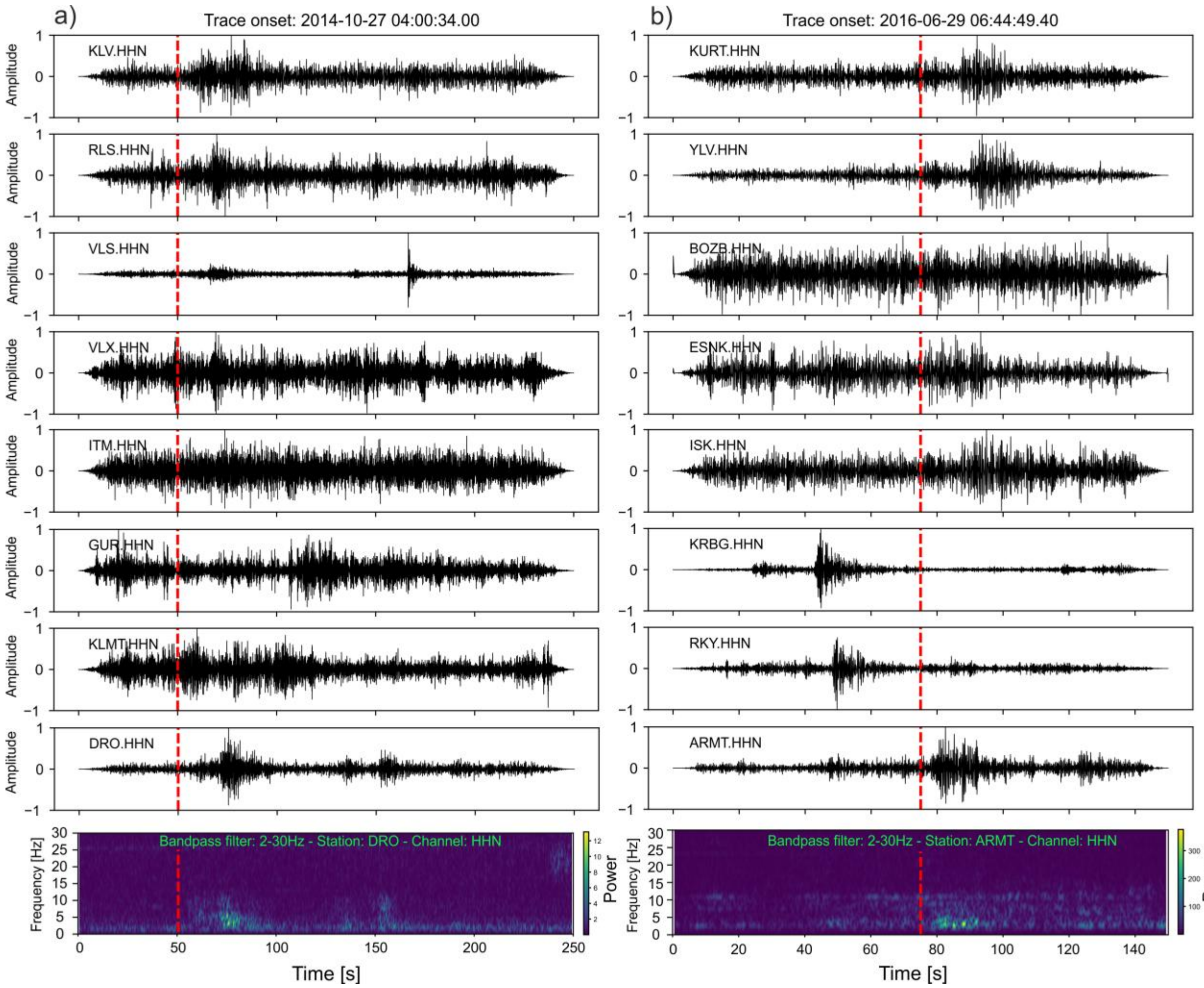

Figure 5. *Example of detected signals using the automatic cross correlation method at the Hellenic Subduction Zone (a) and in the eastern Marmara Sea along the North Anatolian Fault (b). The red line shows the detection time of the signal which does not correspond to the origin time. The bottom panels show the spectrogram of the detected signals shown in the panels above them. The signals are detected by using half-overlapping windows of 300 sec and a cross correlation value of 0.6 at 5 or more channels at stations located <100 km apart. Amplitudes are normalized (-1, 1). All traces are bandpass filtered between 2-8 Hz. Station location is shown in Figure 1S.*

5 Discussion

The most prominent worldwide reported examples of ambient and triggered tremor are primarily limited to fault systems or plate bounding faults located along the Pacific rim (Wech and Creager, 2008; Brown et al., 2009; Ide, 2012; Wech, 2016). The Oriente Fault in Cuba represents, to date, the only exception (Peng et al., 2013) to the above correlation. The results presented here suggest that the lack of deep tremor evidence outside of the Pacific rim point to a requirement that specific conditions may be needed for tremor genesis. In the following, we discuss similarities and differences between the Pacific and the Mediterranean regions to better understand the most relevant conditions for tremor genesis. Although the station coverage is less dense compared to some regions where tremor is observed, it is nevertheless sufficient to observe triggered tremor in the study regions in which we focus, should it occur. Triggered tremor has been recorded at stations more than 100 km apart (Peng et al., 2009), a significantly wider station spacing than used in all four study regions in this work. One limitation of the triggered tremor analysis could be the short time period of investigation, particularly in cases where hypothetical ETS episodes would have longer inter-event periods (for example, if they were to exceed 10 years in the other three regions). The relation between background and triggered tremor is still poorly understood (Chao et al., 2012a), however, many documented cases suggest that tremor is commonly triggered by low stress perturbations (slightly larger than, or similar to tidal stresses e.g. Thomas et al., 2009; Houston, 2015) in areas where ambient tremor occurs, and the time windows considered should be ample to detect triggered tremor. For instance, along the Simi Valley segment of the San Andreas Fault in southern California, where no unambiguous case of ambient tremor is documented, apparent triggering threshold are suggested to be much larger than those for the Parkfield–Cholame section of the San Andreas Fault (>∼12 kPa and 2–3 kPa, respectively; Yang and Peng, 2013), where ambient tremor occurs. Another limitation could be the relatively low PGV_{obs} values recorded in our study regions with respect to circum-Pacific fault systems where tremor occurs, that lie closer to the sources of M>7-7.5 earthquakes. However, we note that the 0.1 cm/s threshold is exceeded during 4-5 events, or 3 events considering a 20 sec period, within each region (Fig. 3a-d), and the estimated dynamic stresses perturbations are > 9 kPa. Therefore, many of what appear to be the important physical criteria associated with observed cases of triggering are met by the candidate mainshocks here. Thus, working on the assumption that the mainshocks generated stress perturbations sufficient to trigger tremor, in the following, we discuss possible causes of absence of tremor in the investigated subduction (5.1) and transform fault systems (5.2).

5.1. Absence of tremor along the Calabrian and the Hellenic Arc

The most striking difference between the Pacific subduction zones and the Mediterranean subduction zones is arguably the age of the down-going plate (Fig. 1, Müller et al., 2008). In addition, relevant differences are represented by the accretionary prisms, with those in the

Mediterranean Sea being wider and thicker (Clift and Vannucchi, 2004), and by the convergence rates, which are on average lower within the Mediterranean basin (Matthews et al., 2016).

The age of the down-going slab controls the thermal state of subducting plate with older slabs being colder and younger slabs being warmer (Peacock and Wang, 1999). Young slabs dehydrate at shallower depths while older slabs dehydrate at greater depth, resulting in significant differences in subduction dynamics (Peacock and Wang, 1999). For instance, in warmer subduction zones (e.g. Cascadia, Mexico, Nankai), the brittle-plastic transition (assumed to be near the 350° C isotherm) occurs at shallower depths (Fig. 2a-b; Peacock and Wang, 1999), and the mantle wedge corner is more hydrated (Abers et al., 2017) relative to older subduction zones (Fig. 6). Thermal models for the Hellenic subduction zone show that the 350° isotherm lies at ~60 km depth (Bocchini et al., 2018; Halpaap et al., 2019), well-below the down-dip limit of the seismogenic zone south of Crete and the intersection between the down-going plate and the overriding plate Moho (Fig. 6b). Although the intersection between the upper-plate Moho and the down-going slab south of Crete is not well-defined, it is not located far from the southern coastline of the Island (Bohnhoff et al., 2001). Hence, the absence of deep tremor is not surprising if we expect it to occur when the down-dip limit of the megathrust is shallower than the slab upper-plate Moho intersection depth (Fig 6a; Gao and Wang, 2017).

A similar situation can be hypothesized for the Calabrian arc, due to the similar age of the subducting slab and its intersection with the upper-plate Moho at ~25 km. In fact, thermal models suggest that the 350° isotherm occurs at depths much greater than 25 km (Fig. 2b) (Syracuse et al., 2010). However, although not in oceanic crust as old as the Mediterranean oceanic lithosphere (>220-230 Ma), tremor does occur at subduction zones where the down-going slab is older than 100 Ma. Examples are the Hikurangi trench in New Zealand (Ide, 2012) and the NE Japan Trench (Nishikawa et al., 2019), where both have common, unique conditions that may prime them for the occurrence of tremor. For instance, deep tremorgenic conditions in New Zealand are explained to be consequence of the high frictional heating along the megathrust that shifts the brittle-plastic transition at depths shallower than that of the upper-plate Moho (Yabe et al., 2014; Gao and Wang, 2017). In NE Japan, tremor occurs at seismogenic depths where tremorgenic conditions are promoted by frictional heterogeneities likely induced by pore fluid changes, sea floor roughness, and/or fracturing of the upper-plate (Nishikawa et al., 2019). We note that in the latter case, tremor at seismogenic depths may be viewed as a special case, as it does not fulfill the definition of deep tremor outlined at the beginning of the paper. In addition, we note another unique example involving the subduction of fluid rich sediments, which is also invoked to explain the deep tremor sources at the eastern termination of the Alaskan subduction zone (at 60-80 km), to date the deepest, well recorded example of tremor worldwide (Wech, 2016).

Very likely there are no anomalous physical conditions present at the Hellenic and Calabrian subduction zones that would be able to create a tremorgenic environment. For instance heat flow values offshore south of Crete (20-30 mW/m2; Eckstein, 1978), as well as in continental Calabria (~40 mW/m2; Loddo et al., 1973) are comparatively low and consistent with the age of the subducting slab, hence excluding the presence of a warm, strong megathrust as in the case of Hikurangi (Gao and Wang, 2014). The mantle wedge corner at both subduction zones is expected to be poorly hydrated due to the old nature of the subducting lithosphere (Abers et al., 2017; Halpaap et al., 2019). In addition, the mantle wedge corner beneath Crete is expected to be poorly hydrated because the current subduction configuration was reached only 15-20 Ma ago (Thomson et al., 1999). It has been proposed that temperature-dependent silica precipitation by upward migrating fluid derived from the down-going slab, by reducing permeability in the forearc crust, favor fluid overpressures and therefore deep tremorgenic conditions (Audet and Bürgmann, 2014). The potential for silica-rich fluids exists in subduction zones where conditions favor high temperatures (Manning, 1997) and it is greatly enhanced by complete serpentinization of the mantle wedge corner (Audet and Bürgmann, 2014). At both the analyzed subduction zones such conditions are not met.

The role that the very thick layer of sediments on the down-going plate could play is not easy to address. ETS episodes are observed in erosional (e.g. Mexico) as well as in accretional (e.g. Cascadia or Nankai) subducting margins (Clift and Vannucchi, 2004). Sediments are water rich and can carry it down, up to 200 km depth. However, they release a considerably smaller amount of water than other slab dehydration sources (van Keken et al., 2011), therefore are not expected to significantly contribute to the hydration of the mantle wedge corner.

With respect to the low geodetic locking depth at both the Hellenic (Vernant et al., 2014) and the Calabrian subduction zones (Pérouse et al., 2012), previous studies suggest that variation of geodetic locking is not correlated to the distribution of deep tremor (Brown et al., 2013).

Therefore, we do not consider the low geodetic locking as relevant to prevent the occurrence of tremor. At the Calabrian Arc, the very low convergence rate may affect the occurrence of tremor, as tremor is not observed elsewhere fault systems moving slower than 5 mm/yr. We note the convergence rates at the Hellenic subduction zone are comparable to those of the slower subduction margins where tremor is observed (e.g. Cascadia, Hikurangi), therefore should not prevent tremor occurrence.

This study does not exclude that tremor could occur above the up-dip limit of the seismogenic zone. The presence of widespread mud volcanos between the backstop and the accretionary wedges of both the Calabrian (Panieri et al., 2013) and Hellenic (Huguen et al., 2001) subduction zones hints at large amounts of fluids released by sediments. High pore fluid pressure could promote tremorgenic conditions above the up-dip limit of the seismogenic zone (Saffer and Wallace, 2015). As already stated, we do not observe any coherent tremor-like signal during surface wave shaking of large mainshocks which suggests the absence of such signals also from different locations other than the down-dip limit of the seismogenic zone. However, as in case of Crete, the up-dip limit of the seismogenic zone is located ~50-60 km to the south of the island (Meier et al., 2004), therefore it could be difficult to observe low amplitude signals at land stations. To rule out or confirm the occurrence of tremor at shallower depths than those expected for the ETS zone, the deployment of dense Ocean Bottom Seismometer networks, as for instance in NE Japan (Nishikawa et al., 2019), would be needed.

Very recently SSEs have been found at the down-dip limit of the seismogenic zone, at depths of 20-40 km beneath western Peloponnese (Mouslopoulou et al., 2020) leaving open the possibility that they may even occur along other segments of the Hellenic Subduction Zone (Saltogianni et al., 2020). The limitation of publicly available geodetic data may have prevented their detection elsewhere. The duration, location and the equivalent moment magnitude released are consistent with those of long-term SSEs (Obara and Kato, 2016). Long-term SSEs are suggested to be manifestation of semi-brittle more towards viscous behavior and are not commonly associated with tremor (Gao and Wang, 2017). In contrast, semi-brittle more towards brittle behavior is invoked to explain ETS episodes (Gao and Wang, 2017). The observations of long-term SSEs at the Hellenic Subduction Zone may suggest the more widespread conditions for long-term SSEs occurrence with respect to that required for ETS episodes (Bürgmann, 2018).

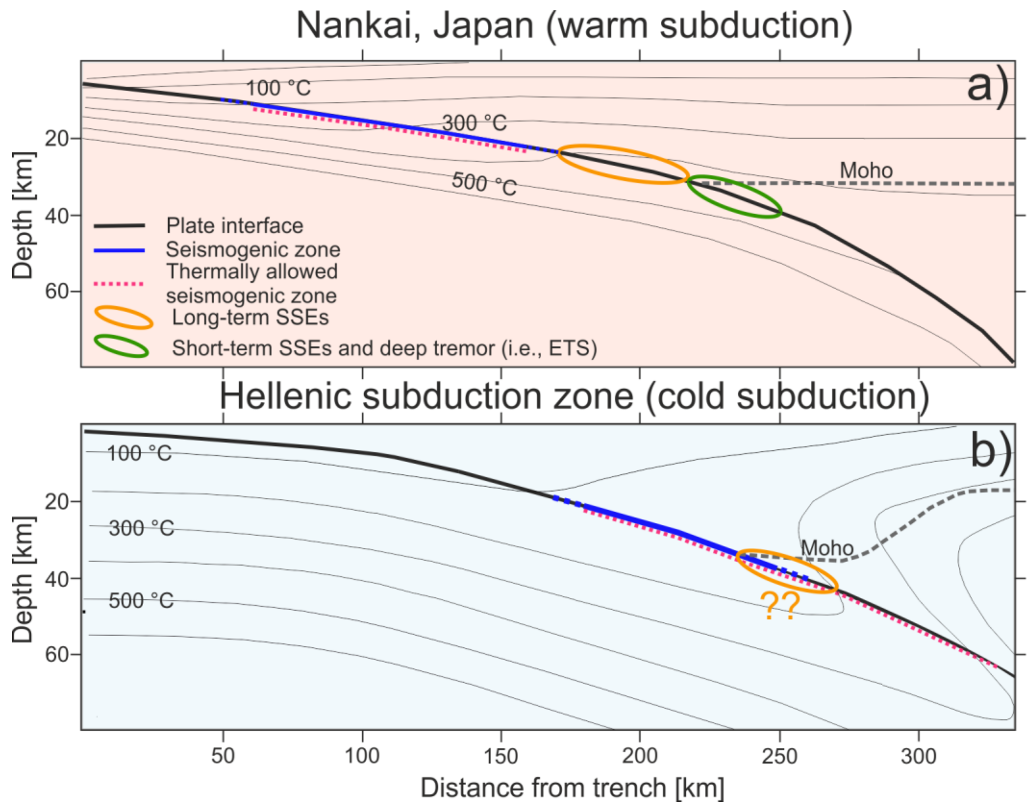

Figure 6. *Sketch comparing typical slip behavior in a (a) warm subduction zone and a (b) cold subduction zone. (a) Cross-section along the Nankai trench (Japan) adapted from Gao and Wang (2017). (b) Cross-section across Crete using slab geometry and thermal structure from half-space cooling model in Bocchini et al. (2018). Upper-plate Moho depth in subfigure b from available active and passive seismological studies (Bohnhoff et al., 2001; Meier et al., 2007).*

5.2. Absence of tremor along the Kefalonia Transform Fault and North Anatolia Fault in the Sea of Marmara

Of the documented cases of tremor along transform margins, the most well-established examples are for the Parkfield-Cholame segment of the San Andreas Fault (Nadeau and Dolenc, 2005; Peng et al., 2009, Shelly, 2017). The occurrence of tremor in the Parkfield-Cholame area is interpreted to be related to the presence of remnants of partially serpentinized mantle wedge from a former subduction zone (Kirby et al., 2014). The frequency of tremor episodes significantly decreases towards NW (Calaveras) and SE (San Jacinto) along the SAF (Gomberg et al., 2008; Peng et al., 2009) enhancing the primary control exerted by the water reservoir beneath the Parkfield-Cholame segment. Although less frequent, deep tremor activity beneath the Alpine Fault in New Zealand is also related to the presence of high pore fluid pressures (Wech et al., 2012). Along the Kefalonia Fault and the North Anatolian Fault segment in the Sea of Marmara, such a fluid source is possibly missing and/or do not exist the conditions to create high fluid pressures to promote tremorgenesis. Our results along the North Anatolian Fault are consistent with those of Pfohl et al. (2015) that found no unambiguous evidence for triggered or ambient tremor along the central segment of the North Anatolian Fault. In addition, the transtensional regime in the Sea of Marmara may also not be favorable for tremor occurrence, as most observations of tremor occur along compressive or transform/transpressive margins (Fig. 1). While the Kefalonia Transform Fault exhibits transpressional deformation like the Alpine and San Andreas Faults, it shows a different tectonic evolution. For example, it is not located along a former suture zone and it is much younger, with less accumulated displacement (van Hinsbergen et al., 2006). Furthermore, the seismogenic layer and the Moho depths do not occur at anomalous depths at either the Kefalonia Transform Fault as well as at the Çınarcık segment of the North Anatolian Fault (section 2.1 and section 2.4) that could hint at significantly high or low temperature gradients.

The absence of triggered tremor in the eastern Marmara Sea agrees with the absence of LFE/tremor activity accompanying the ~50-daylong SSE along the Çınarcık fault (Martínez-Garzón et al., 2019). The absence of ambient tremor would imply that the SSE could have either occurred at shallow depth, consistently to adjacent segments of the North Anatolian Fault (Aslan et al., 2019; Rousset et al., 2016) or if at the down-dip limit of the seismogenic zone, to exhibit similar characteristics of the long-term SSEs that are observed to be not strongly correlated with the occurrence of tremor (Husker et al., 2012; Obara, 2011). The occurrence of shallow SSE along adjacent segments of the North Anatolian Fault would support the shallow origin of the signal.

6 Conclusions

We find no unambiguous evidence for triggered deep tremor at the Hellenic Subduction Zone, beneath Crete, at the Calabrian Subduction Zone, at the Kefalonia Transform Fault, and at the North Anatolian Fault, in the eastern Marmara Sea, during the passage of surface waves of 16-18 teleseismic events between 2010 and 2020. Furthermore, we find no unambiguous examples of LFE/tremor activity accompanying the SSE in the eastern Marmara Sea and the two SSEs beneath Peloponnese, along the western segment of the Hellenic Subduction Zone. The absence of tremor along the North Anatolian Fault agrees with the findings from a previous study. The absence of triggered tremor, strengthened by the absence of ambient tremor during

SSE episodes, suggests the absence of favorable physical conditions for a deep ETS zone in the central-eastern Mediterranean basin. The results confirm the significant influence of the slab thermal structure on the occurrence of deep tremor in subduction zones. The very old and cold slabs at the Calabrian and Hellenic subduction zones do not favor tremorgenesis. The possible absence of fluid sources, able to promote elevated pore fluid pressures at the base of the seismogenic layers at the Kefalonia and North Anatolian transform faults could explain the absence of tremor. In addition, the transtensional regime within the Çınarcık basin, in the eastern Sea of Marmara, does not seem favorable to the generation of tremor. The absence of LFEs/tremor activity accompanying the SSE along the Çınarcık Fault in the eastern Sea of Marmara would suggest that the detected ~50-daylong SSE occurred either at shallow depths in agreement with observations from adjacent segments, or that, if deep, could be classified as long-term SSE. The depth range, duration, and absence of tremor during the SSEs along the western segment of the Hellenic Subduction Zone are also consistent with those of long-term SSEs observed elsewhere. The absence of deep tremor indicate the more widespread conditions for the occurrence of long-term SSEs, likely a manifestation of semi-brittle more towards viscous behavior, compared to that suggested for ETS that require a restoration of a brittle or semi-brittle regime at depths where under normal condition rocks would deform viscously.

Acknowledgments, Samples, and Data

G.M.B has been funded with Ruhr Uuniversity of Bochum new faculty startup funds awarded to R.M.H.. P.M-G. acknowledges funding from the Helmholtz Young Investigators Group: SAIDAN (VH-NG-1323). We are grateful to the Institute of Geodynamics of the National Observatory of Athens (NOA, Greece) and all partners of the Hellenic Unified Seismic Network, including the University of Patra, University of Thessaloniki and University of Athens, to the Technological Educational Institute of Crete (Greece), to INGV (Italy), to KOERI (Turkey) technical staff for the installation and maintenance of seismic networks and for publicly sharing data. Data from such networks used in this study are freely accessible from EIDA database. Thanks to the Turkish Disaster and Emergency Management Presidency (AFAD) in Ankara for providing waveform data from the GONAF observatory. Access to the GONAF and PIRES networks is granted upon request to Marco Bohnhoff (GFZ). Many thanks to Yajing Liu for her constructive comments on a draft of the manuscript and to Satoshi Ide for having shared the envelope cross-correlation code for ambient tremor detection. Figures were realized using the Global Mapping Tool (Wessel et al., 2013) and matplotlib. Waveform data processing was performed with Obspy.

References

Abers, G.A., Van Keken, P.E., & Hacker, B.R. (2017), The cold and relatively dry nature of mantle forearcs in subduction zones. *Nature Geosciences*. https://doi.org/10.1038/ngeo2922

Aiken, C., Peng, Z., & Chao, K. (2013), Tremors along the Queen Charlotte Margin triggered by large teleseismic earthquakes. *Geophysical Research Letters*. https://doi.org/10.1002/grl.50220

Aki, K., & Richards, P.G. (2002), Quantitative seismology.

Armijo, R., Meyer, B., Navarro, S., King, G., & Barka, A. (2002), Asymmetric slip partitioning in the sea of Marmara pull-apart: A clue to propagation processes of the North Anatolian Fault? *Terra Nova*. https://doi.org/10.1046/j.1365-3121.2002.00397.x

Aslan, G., Lasserre, C., Cakir, Z., Ergintav, S., Özarpaci, S., Dogan, U., Bilham, R., & Renard, F. (2019), Shallow Creep Along the 1999 Izmit Earthquake Rupture (Turkey) From GPS and High Temporal Resolution Interferometric Synthetic Aperture Radar Data (2011–2017). *Journal Geophysical Research: Solid Earth*. https://doi.org/10.1029/2018JB017022

Audet, P., Bostock, M.G., Christensen, N.I., & Peacock, S.M. (2009), Seismic evidence for overpressured subducted oceanic crust and megathrust fault sealing. *Nature,* 457, 76–78. https://doi.org/10.1038/nature07650

Audet, P., & Bürgmann, R. (2014), Possible control of subduction zone slow-earthquake periodicity by silica enrichment. *Nature*. https://doi.org/10.1038/nature13391

Audet, P., & Kim, Y.H. (2016), Teleseismic constraints on the geological environment of deep episodic slow earthquakes in subduction zone forearcs: A review. *Tectonophysics*. https://doi.org/10.1016/j.tecto.2016.01.005

Becker, D., & Meier, T. (2010), Seismic slip deficit in the southwestern forearc of the hellenic subduction zone. *Bulletin of the Seismological Society of America*, 100, 325–342. https://doi.org/10.1785/0120090156

Bocchini, G.M., Brüstle, A., Becker, D., Meier, T., van Keken, P.E., Ruscic, M., Papadopoulos, G.A., Rische, M., & Friederich, W. (2018), Tearing, segmentation, and backstepping of subduction in the Aegean: New insights from seismicity. *Tectonophysics*, 734–735, 96–118. https://doi.org/10.1016/j.tecto.2018.04.002

Bockholt, B.M., Langston, C.A., Horton, S., Withers, M., & Deshon, H.R. (2014), Mysterious tremor-like signals seen on the reelfoot fault, Northern Tennessee. *Bulletin Seismological Society of America*. https://doi.org/10.1785/0120140030

Bohnhoff, M., Dresen, G., Ceken, U., Kadirioglu, F.T., Kartal, R.F., Kilic, T., Nurlu, M., Yanik, K., Acarel, D., Bulut, F., Ito, H., Johnson, W., Malin, P.E., & Mencin, D. (2017), GONAF - The borehole geophysical observatory at the North Anatolian Fault in the eastern Sea of Marmara. *Scientific Drilling*. https://doi.org/10.5194/sd-22-19-2017

Bohnhoff, M., Makris, J., Papanikolaou, D., & Stavrakakis, G. (2001), Crustal investigation of the Hellenic subduction zone using wide aperture seismic data. *Tectonophysics*, 343, 239–262. https://doi.org/10.1016/S0040-1951(01)00264-5

Bohnhoff, M., Martínez-Garzón, P., Bulut, F., Stierle, E., & Ben-Zion, Y. (2016), Maximum earthquake magnitudes along different sections of the North Anatolian fault zone. *Tectonophysics*. https://doi.org/10.1016/j.tecto.2016.02.028

Brown, J.R., Beroza, G.C., Ide, S., Ohta, K., Shelly, D.R., Schwartz, S.Y., Rabbel, W., Thorwart, M., & Kao, H. (2009), Deep low-frequency earthquakes in tremor localize to the plate interface in multiple subduction zones. *Geophysical Research Letters.* https://doi.org/10.1029/2009GL040027

Brown, J.R., Prejean, S.G., Beroza, G.C., Gomberg, J.S., & Haeussler, P.J. (2013), Deep low-frequency earthquakes in tectonic tremor along the Alaska-Aleutian subduction zone. *Journal of Geophysical Research: Solid Earth*. https://doi.org/10.1029/2012JB009459

Bürgmann, R., (2018), The geophysics, geology and mechanics of slow fault slip. *Earth and Planetary Science Letters.* https://doi.org/10.1016/j.epsl.2018.04.062

Carafa, M.M.C., Kastelic, V., Bird, P., Maesano, F.E., & Valensise, G. (2018), A "Geodetic Gap" in the Calabrian Arc: Evidence for a Locked Subduction Megathrust?. *Geophysical Research Letters*. https://doi.org/10.1002/2017GL076554

Carton, H., Singh, S.C., Hirn, A., Bazin, S., de Voogd, B., Vigner, A., Ricolleau, A., Cetin, S., Oçakoğlu, N., Karakoç, F., & Sevilgen, V. (2007), Seismic imaging of the three-dimensional architecture of the Çınarcık Basin along the North Anatolian Fault. *Journal of Geophysical Research: Solid Earth*. https://doi.org/10.1029/2006JB004548

Chamberlain, C.J., Hopp, C.J., Boese, C.M., Warren-Smith, E., Chambers, D., Chu, S.X., Michailos, K., & Townend, J. (2018), EQcorrscan: Repeating and near-repeating earthquake detection and analysis in python. *Seismological Research Letters.* https://doi.org/10.1785/0220170151

Chao, K., Peng, Z., Fabian, A., & Ojha, L. (2012a), Comparisons of triggered tremor in California. *Bulletin of the Seismological Society of America.* https://doi.org/10.1785/0120110151

Chao, K., Peng, Z., Gonzalez-Huizar, H., Aiken, C., Enescu, B., Kao, H., Velasco, A.A., Obara, K., & Matsuzawa, T. (2013), A Global search for triggered tremor following the 2011 Mw 9.0 Tohoku earthquake. *Bulletin of the Seismological Society of America.* https://doi.org/10.1785/0120120171

Chao, K., Peng, Z., Wu, C., Tang, C.C., & Lin, C.H. (2012b), Remote triggering of non-volcanic tremor around Taiwan. *Geophysical Jornal International.* https://doi.org/10.1111/j.1365-246X.2011.05261.x

Clift, P., &Vannucchi, P. (2004), Controls on tectonic accretion versus erosion in subduction zones: Implications for the origin and recycling of the continental crust. *Reviews Geophysics.* https://doi.org/10.1029/2003RG000127

de Voogd, B., Truffert, C., Chamot-Rooke, N., Huchon, P., Lallemant, S., Le Pichon, X., (1992), Two-ship deep seismic soundings in the basins of the Eastern Mediterranean Sea (Pasiphae cruise). *Geophysical Jornal International.* https://doi.org/10.1111/j.1365-246X.1992.tb00116.x

Dickinson, W.R., & Wernicke, B.P. (1997), Reconciliation of San Andreas slip discrepancy by a combination of interior basin and range extension and transrotation near the coast. *Geology*. https://doi.org/10.1130/0091-7613(1997)025<0663:ROSASD>2.3.CO;2

Eckstein, Y. (1978), Review of heat flow data from the eastern Mediterranean region. *Pure Applied Geophysics*, 117, 150–159.

Faccenna, C., Becker, T.W., Auer, L., Billi, A., Boschi, L., Brun, J.P., Capitanio, F.A., Funiciello, F., Horvàth, F., Jolivet, L., Piromallo, C., Royden, L., Rossetti, F., & Serpelloni, E. (2014), Mantle dynamics in the Mediterranean. *Reviews Geophysics,* 52, 283–332. https://doi.org/10.1002/2013RG000444.Received

Faccenna, C., Funiciello, F., Giardini, D., & Lucente, P. (2001), Episodic back-arc extension during restricted mantle convection in the Central Mediterranean. *Earth and Planetary Science Letters.* https://doi.org/10.1016/S0012-821X(01)00280-1

Fry, B., Chao, K., Bannister, S., Peng, Z., & Wallace, L. (2011), Deep tremor in New Zealand triggered by the 2010 Mw8.8 Chile earthquake. *Geophysical Research Letters.* https://doi.org/10.1029/2011GL048319

Gao, X., & Wang, K. (2014), Strength of stick-slip and creeping subduction megathrusts from heat flow observations. *Science* (80-.). https://doi.org/10.1126/science.1255487

Gao, X., & Wang, K. (2017), Rheological separation of the megathrust seismogenic zone and episodic tremor and slip. *Nature.* https://doi.org/10.1038/nature21389

GFZ Potsdam, BU-Kandilli (2006), Prince Islands Real-time Earthquake monitoring System. International Federation of Digital Seismograph Networks. Dataset/Seismic Network. https://doi.org/10.7914/SN/PZ

Ghosh, A., Vidale, J.E., Peng, Z., Creager, K.C., Houston, H. (2009a), Complex nonvolcanic tremor near Parkfield, California, triggered by the great 2004 Sumatra earthquake. *Journal of Geophysical Research: Solid Earth*. https://doi.org/10.1029/2008JB006062

Ghosh, A., Vidale, J.E., Sweet, J.R., Creager, K.C., & Wech, A.G. (2009b), Tremor patches in Cascadia revealed by seismic array analysis. *Geophysical Research Letters.* https://doi.org/10.1029/2009GL039080

Gomberg, J., Rubinstein, J.L., Peng, Z., Creager, K.C., Vidale, J.E., & Bodin, P. (2008), Widespread triggering of nonvolcanic tremor in California. *Science* (80-.).

https://doi.org/10.1126/science.1149164

Granot, R. (2016), Palaeozoic oceanic crust preserved beneath the eastern Mediterranean. *Nature Geoscience*, 9, 701–705. https://doi.org/10.1038/ngeo2784

Guidoboni, E., & Comastri, A. (2005), Catalogue of earthquakes and tsunamis in the Mediterranean area from the 11th to the 15th century. Rome : Istituto nazionale di geofisica e vulcanologia.

Halpaap, F., Rondenay, S., Perrin, A., Goes, S., Ottemöller, L., Austrheim, H., Shaw, R., & Eeken, T. (2019), Earthquakes track subduction fluids from slab source to mantle wedge sink. *Science Advances*. https://doi.org/10.1126/sciadv.aav7369

Houston, H. (2015), Low friction and fault weakening revealed by rising sensitivity of tremor to tidal stress. *Nature Geoscience.* https://doi.org/10.1038/ngeo2419

Huguen, C., Mascle, J., Chaumillon, E., Woodside, J.M., Benkhelil, J., Kopf, A., & Volkonskaïa, A. (2001), Deformational styles of the Eastern Mediterranean ridge and surroundings from combined swath mapping and seismic reflection profiling. *Tectonophysics*, 343, 21–47. https://doi.org/10.1016/S0040-1951(01)00185-8

Husker, A.L., Kostoglodov, V., Cruz-Atienza, V.M., Legrand, D., Shapiro, N.M., Payero, J.S., Campillo, M., & Huesca-Pérez, E. (2012), Temporal variations of non-volcanic tremor (NVT) locations in the Mexican subduction zone: Finding the NVT sweet spot. *Geochemistry, Geophysics and Geosystems.* https://doi.org/10.1029/2011GC003916

Ide, S. (2010), Striations, duration, migration and tidal response in deep tremor. *Nature*. https://doi.org/10.1038/nature09251

Ide, S. (2012), Variety and spatial heterogeneity of tectonic tremor worldwide. *Journal of Geophysical Research: Solid Earth*. https://doi.org/10.1029/2011JB008840

ISC, International Seismological Centre (2020), On-line Bulletin. https://doi.org/10.31905/D808B830

Ito, Y., Obara, K., Shiomi, K., Sekine, S., & Hirose, H. (2007), Slow earthquakes coincident with episodic tremors and slow slip events. *Science* (80-.). https://doi.org/10.1126/science.1134454

Jenkins, J., Stephenson, S.N., Martínez-Garzón, P., Bohnhoff, M., & Nurlu, M. (2020), Crustal thickness variation across the Sea of Marmara region, NW Turkey: a reflection of modern and ancient tectonic processes. *Tectonics*. https://doi.org/10.1029/2019TC005986

Kennett, B.L.N., & Engdahl, E.R. (1991), Traveltimes for global earthquake location and phase identification. *Geophysical Journal International*. https://doi.org/10.1111/j.1365-246X.1991.tb06724.x

Kim, M.J., Schwartz, S.Y., & Bannister, S. (2011), Non-volcanic tremor associated with the

March 2010 Gisborne slow slip event at the Hikurangi subduction margin, New Zealand. *Geophysical Research Letters*. https://doi.org/10.1029/2011GL048400

Kirby, S.H., Wang, K., & Brocher, T.M. (2014), A large mantle water source for the northern san andreas fault system: A ghost of subduction past. *Earth, Planets and Space*. https://doi.org/10.1186/1880-5981-66-67

Kodaira, S., Iidaka, T., Kato, A., Park, J.O., Iwasaki, T., & Kaneda, Y. (2004), High pore fluid pressure may cause silent slip in the Nankai Trough. *Science* (80-.). https://doi.org/10.1126/science.1096535

Lay, T., & Wallace, T.C. (1995), Modern global seismology. Elsevier.

Le Pichón, X., Şeng Ör, A.M.C., Kende, J., İmren, C., Henry, P., Grail, C., & Karabulut, H. (2016), Propagation of a strike-slip plate boundary within an extensional environment: The westward propagation of the North Anatolian fault. *Canadian Journal of Earth Sciences*. https://doi.org/10.1139/cjes-2015-0129

Loddo, M., Mongelli, F., & Roda, C. (1973), Heat flow in Calabria, Italy. *Nature Physics Science,* 244, 91–92.

Louvari, E., Kiratzi, A.A., & Papazachos, B.C. (1999), The Cephalonia Transform Fault and its extension to western Lefkada Island (Greece). *Tectonophysics,* 308, 223–236. https://doi.org/10.1016/S0040-1951(99)00078-5

Maesano, F.E., Tiberti, M.M., & Basili, R. (2017), The Calabrian Arc: Three-dimensional modelling of the subduction interface. *Scientific Reports*. https://doi.org/10.1038/s41598-017-09074-8

Malin, P.E., Bohnhoff, M., Blümle, F., Dresen, G., Martínez-Garzón, P., Nurlu, M., Ceken, U., Kadirioglu, F.T., Kartal, R.F., Kilic, T., & Yanik, K. (2018), Microearthquakes preceding a M4.2 Earthquake Offshore Istanbul. *Scientific Reports*. https://doi.org/10.1038/s41598-018-34563-9

Manning, C.E. (1997), Coupled Reaction and Flow in Subduction Zones: Silica Metasomatism in the Mantle Wedge. In: Fluid Flow and Transport in Rocks. https://doi.org/10.1007/978-94-009-1533-6_8

Martínez-Garzón, P., Bohnhoff, M., Mencin, D., Kwiatek, G., Dresen, G., Hodgkinson, K., Nurlu, M., Kadirioglu, F.T., & Kartal, R.F. (2019), Slow strain release along the eastern Marmara region offshore Istanbul in conjunction with enhanced local seismic moment release. *Earth and Planetary Science Letters*. https://doi.org/10.1016/j.epsl.2019.01.001

Martínez-Garzón, P., Heidbach, O., & Bohnhoff, M. (2020), Contemporary stress and strain field in the Mediterranean from stress inversion of focal mechanisms and GPS data. *Tectonophysics*, 774, 228286.

Matthews, K.J., Maloney, K.T., Zahirovic, S., Williams, S.E., Seton, M., & Müller, R.D. (2016), Global plate boundary evolution and kinematics since the late Paleozoic. *Global and Planetary Change*. https://doi.org/10.1016/j.gloplacha.2016.10.002

McClusky, S., Balassanian, S., Barka, A., Demir, C., Ergintav, S., Georgiev, I., Gurkan, O., Hamburger, M., Hurst, K., Kahle, H., Kastens, K., Kekelidze, G., King, R., Kotzev, V., Lenk, O., Mahmoud, S., Mishin, A., Nadariya, M., Ouzounis, A., Paradissis, D., Peter, Y., Prilepin, M., Reilinger, R., Sanli, I., Seeger, H., Tealeb, A., Toksöz, M.N., & Veis, G. (2000), Global Positioning System constraints on plate kinematics and dynamics in the eastern Mediterranean and Caucasus. *Journal of Geophysical Research: Solid Earth*, 105, 5695–5719. https://doi.org/10.1029/1999JB900351

Meier, T., Becker, D., Endrun, B., Rische, M., Bohnhoff, M., Stöckhert, B., & Harjes, H.-P. (2007), A model for the Hellenic subduction zone in the area of Crete based on seismological investigations, in: Taymaz, T., Yilmaz, Y., Dilek, Y. (Eds.), The Geodynamic of the Aegean and Anatolia. *Geological Society, London, Special Publications*, 183–199. https://doi.org/10.1144/SP291.9

Meier, T., Rische, M., Endrun, B., Vafidis, A., & Harjes, H.-P. (2004), Seismicity of the Hellenic subduction zone in the area of western and central Crete observed by temporary local seismic networks. *Tectonophysics*, 383, 149–169. https://doi.org/10.1016/j.tecto.2004.02.004

Miyazawa, M., & Brodsky, E.E. (2008), Deep low-frequency tremor that correlates with passing surface waves. *Journal of Geophysical Research: Solid Earth.* https://doi.org/10.1029/2006JB004890

Miyazawa, M., Brodsky, E.E., & Mori, J. (2008), Learning from dynamic triggering of low-frequency tremor in subduction zones. *Earth, Planets and Space.* https://doi.org/10.1186/BF03352858

Mouslopoulou, V., Bocchini, G.M., Cesca, S., Saltogianni, V., Bedford, J.R., Petersen, G.M., Gianniou, M., & Oncken, O. (2020), Earthquake-swarms, slow-slip and fault-interactions at the western-end of the Hellenic Subduction System precede the Mw 6.9 Zakynthos Earthquake, Greece. *Earth and Space Science Open Archive.* https://doi.org/10.1002/essoar.10503389.1

Müller, R.D., Sdrolias, M., Gaina, C., & Roest, W.R. (2008), Age, spreading rates, and spreading asymmetry of the world's ocean crust. *Geochemistry, Geophys. Geosystems*, 9. https://doi.org/10.1029/2007GC001743

Nadeau, R.M., & Dolenc, D. (2005), Nonvolcanic tremors deep beneath the San Andreas Fault. *Science* (80-.). https://doi.org/10.1126/science.1107142

Nishikawa, T., Matsuzawa, T., Ohta, K., Uchida, N., Nishimura, T., & Ide, S. (2019), The slow earthquake spectrum in the Japan Trench illuminated by the S-net seafloor observatories. *Science* (80-.). https://doi.org/10.1126/science.aax5618

Norris, R.J., & Cooper, A.F. (2001), Late Quaternary slip rates and slip partitioning on the Alpine Fault, New Zealand. *Journal of Structural Geology*. https://doi.org/10.1016/S0191-

8141(00)00122-X

Obara, K. (2002), Nonvolcanic deep tremor associated with subduction in southwest Japan. *Science* (80-.). https://doi.org/10.1126/science.1070378

Obara, K. (2011), Characteristics and interactions between non-volcanic tremor and related slow earthquakes in the Nankai subduction zone, southwest Japan. *Journal of Geodynamics*. https://doi.org/10.1016/j.jog.2011.04.002

Obara, K., & Kato, A. (2016), Connecting slow earthquakes to huge earthquakes. *Science*. https://doi.org/10.1126/science.aaf1512

Panieri, G., Polonia, A., Lucchi, R.G., Zironi, S., Capotondi, L., Negri, A., & Torelli, L. (2013), Mud volcanoes along the inner deformation front of the Calabrian Arc accretionary wedge (Ionian Sea). *Marine Geology*. https://doi.org/10.1016/j.margeo.2012.11.003

Papadimitriou, E., Karakostas, V., Mesimeri, M., Chouliaras, G., & Kourouklas, C. (2017), The Mw6.5 17 November 2015 Lefkada (Greece) Earthquake: Structural Interpretation by Means of the Aftershock Analysis. *Pure and Applied Geophysics*. https://doi.org/10.1007/s00024-017-1601-3

Papazachos, B.C., & Papazachou, C. (2003), The Earthquakes of Greece. Ziti Publications, Thessaloniki (in Greek).

Peacock, S.M., & Wang, K. (1999), Seismic consequences of warm versus cool subduction metamorphism: Examples from southwest and northeast Japan. *Science* (80-.). 286, 937–939. https://doi.org/10.1126/science.286.5441.937

Peng, Z., & Chao, K. (2008), Non-volcanic tremor beneath the Central Range in Taiwan triggered by the 2001 Mw 7.8 Kunlun earthquake. *Geophysical Journal International*. https://doi.org/10.1111/j.1365-246X.2008.03886.x

Peng, Z., & Gomberg, J. (2010), An integrated perspective of the continuum between earthquakes and slow-slip phenomena. *Nature Geoscience.* https://doi.org/10.1038/ngeo940

Peng, Z., Gonzalez-Huizar, H., Chao, K., Aiken, C., Moreno, B., & Armstrong, G. (2013), Tectonic tremor beneath Cuba triggered by the Mw 8.8 maule and Mw 9.0 tohoku-oki earthquakes. *Bulletin of the Seismological Society of America*. https://doi.org/10.1785/0120120253

Peng, Z., Vidale, J.E., Wech, A.G., Nadeau, R.M., & Creager, K.C. (2009), Remote triggering of tremor along the San Andreas Fault in central California. *Journal of Geophysical Research: Solid Earth*. https://doi.org/10.1029/2008JB006049

Pérouse, E., Chamot-Rooke, N., Rabaute, A., Briole, P., Jouanne, F., Georgiev, I., & Dimitrov, D., (2012), Bridging onshore and offshore present-day kinematics of central and eastern Mediterranean: Implications for crustal dynamics and mantle flow. *Geochemistry, Geophysics and Geosystems.* https://doi.org/10.1029/2012GC004289

Pfohl, A., Warren, L.M., Sit, S., & Brudzinski, M. (2015), Search for tectonic tremor on the central north Anatolian fault, Turkey. *Bulletin of the Seismological Society of America*. https://doi.org/10.1785/0120140312

Rogers, G., & Dragert, H. (2003), Episodic tremor and slip on the Cascadia subduction zone: The chatter of silent slip. *Science* (80-.). https://doi.org/10.1126/science.1084783

Romanet, P., Bhat, H.S., Jolivet, R., & Madariaga, R. (2018), Fast and Slow Slip Events Emerge Due to Fault Geometrical Complexity. *Geophysical Research Letters.* https://doi.org/10.1029/2018GL077579

Rousset, B., Jolivet, R., Simons, M., Lasserre, C., Riel, B., Milillo, P., Çakir, Z., & Renard, F. (2016), An aseismic slip transient on the North Anatolian Fault. *Geophysical Research Letters*. https://doi.org/10.1002/2016GL068250

Rubinstein, J.L., Vidale, J.E., Gomberg, J., Bodin, P., Creager, K.C., & Malone, S.D. (2007), Non-volcanic tremor driven by large transient shear stresses. Nature. https://doi.org/10.1038/nature06017

Ryan, W.B.F., Carbotte, S.M., Coplan, J.O., O'Hara, S., Melkonian, A., Arko, R., Weissel, R.A., Ferrini, V., Goodwillie, A., Nitsche, F., Bonczkowski, J., & Zemsky, R. (2009), Global multi-resolution topography synthesis. *Geochemistry, Geophysics and Geosystems.* https://doi.org/10.1029/2008GC002332

Saffer, D.M., & Wallace, L.M. (2015), The frictional, hydrologic, metamorphic and thermal habitat of shallow slow earthquakes. *Nature Geoscience.* https://doi.org/10.1038/ngeo2490

Saltogianni, V., Mouslopoulou, V., Oncken, O., Nicol, A., Gianniou, M., & Mertikas, S. (2020), Elastic fault interactions and earthquake-rupture along the southern Hellenic subduction plate-interface zone in Greece. *Geophysical Research Letters.* https://doi.org/10.1029/2019GL086604

Scholz, C.H. (1998), Earthquakes and friction laws. *Nature*. https://doi.org/10.1038/34097

Schwartz, S.Y., & Rokosky, J.M. (2007), Circum-Pacific Subduction Zones. *Reviews Geophysics*. https://doi.org/10.1029/2006RG000208.1.

Selvaggi, G., & Chiarabba, C. (1995), Seismicity and P-wave velocity image of the Southern Tyrrhenian subduction zone. *Geophysical Journal International*. https://doi.org/10.1111/j.1365-246X.1995.tb06441.x

Şengör, A.M.., Tüysüz, O., İmren, C., Sakınç, M., Eyidoğan, H., Görür, N., Le Pichon, X., Rangin, C. (2005), The North Anatolian Fault: A New Look. *Annual Reviews of Earth and Planetary Science*. https://doi.org/10.1146/annurev.earth.32.101802.120415

Shelly, D.R., Beroza, G.C., & Ide, S. (2007), Non-volcanic tremor and low-frequency earthquake swarms. Nature. https://doi.org/10.1038/nature05666

Shelly, D.R. (2017), A 15 year catalog of more than 1 million low-frequency earthquakes:

Tracking tremor and slip along the deep San Andreas Fault. *Journal of Geophysical Research: Solid Earth.* https://doi.org/10.1002/2017JB014047

Sodoudi, F., Kind, R., Hatzfeld, D., Priestley, K., Hanka, W., Wylegalla, K., Stavrakakis, G., Vafidis, A., Harjes, H.P., & Bohnhoff, M. (2006), Lithospheric structure of the Aegean obtained from P and S receiver functions. *Journal of Geophysical Research: Solid Earth.* 111. https://doi.org/10.1029/2005JB003932

Speranza, F., Minelli, L., Pignatelli, A., & Chiappini, M. (2012), The Ionian Sea: The oldest in situ ocean fragment of the world? *Journal of Geophysical Research: Solid Earth*, 117, 1–13. https://doi.org/10.1029/2012JB009475

Stein, R.S., Barka, A.A., & Dieterich, J.H. (1997), Progressive failure on the North Anatolian fault since 1939 by earthquake stress triggering. *Geophysical Journal International*. https://doi.org/10.1111/j.1365-246X.1997.tb05321.x

Sun, W.F., Peng, Z., Lin, C.H., & Chao, K. (2015), Detecting deep tectonic tremor in taiwan with a dense array. *Bulletin of the Seismological Society of America.* https://doi.org/10.1785/0120140258

Syracuse, E.M., van Keken, P.E., Abers, G.A., Suetsugu, D., Bina, C., Inoue, T., Wiens, D., & Jellinek, M. (2010), The global range of subduction zone thermal models. *Physics of the Earth and Planetary Interiors,* 183, 73–90. https://doi.org/10.1016/j.pepi.2010.02.004

Thomas, A.M., Nadeau, R.M., & Bürgmann, R. (2009), Tremor-tide correlations and near-lithostatic pore pressure on the deep San Andreas fault. *Nature*. https://doi.org/10.1038/nature08654

Thomson, S.N., Stöckhert, B., & Brix, M.R. (1999), Miocene high-pressure metamorphic rocks of Crete, Greece: rapid exhumation by buoyant escape, in: Ring, U., Lister, G., Willet, S., Brandon, M. (Eds.), Exhumation Processes: Normal Faulting, Ductile Flow, and Erosion. *Geological Society, London, Special Publications,* 154, 87–107. http://dx.doi.org/10.1144/GSL.SP.1999.154.01.04

Tunç, B., Çaka, D., Irmak, T.S., Woith, H., Tunç, S., Bariş, Ş., Özer, M.F., Lühr, B.G., Günther, E., Grosser, H., & Zschau, J. (2011), The Armutlu Network: An investigation into the seismotectonic setting of Armutlu-Yalova-Gemlik and the surrounding regions. *Annals of Geophysics*. https://doi.org/10.4401/ag-4877

van Hinsbergen, D.J.J., van der Meer, D.G., Zachariasse, W.J., & Meulenkamp, J.E. (2006), Deformation of western Greece during Neogene clockwise rotation and collision with Apulia. *International Journal of Earth Sciences,* 95, 463–490. https://doi.org/10.1007/s00531-005-0047-5

van der Elst, N.J., Delorey, A.A., Shelly, D.R., & Johnson, P. A. (2016), Fortnightly modulation of San Andreas tremor and low-frequency earthquakes. *Proceedings of the National Academy of Sciences*, 113(31), 8601–8605. https://doi.org/10.1073/pnas.1524316113 van Keken, P.E., Hacker, B.R., Syracuse, E.M., & Abers, G.A. (2011), Subduction factory: 4. Depth-dependent flux of H2O from subducting slabs worldwide. *Journal of Geophysical Research: Solid Earth*, 116. https://doi.org/10.1029/2010JB007922

Vernant, P., Reilinger, R., & McClusky, S. (2014), Geodetic evidence for low coupling on the Hellenic subduction plate interface. *Earth and Planetary Science Letters*, 385, 122–129. https://doi.org/10.1016/j.epsl.2013.10.018

Wallace, L.M., Beavan, J., Bannister, S., & Williams, C. (2012), Simultaneous long-term and short-term slow slip events at the Hikurangi subduction margin, New Zealand: Implications for processes that control slow slip event occurrence, duration, and migration. *Journal of Geophysical Research Solid Earth*. https://doi.org/10.1029/2012JB009489

Walter, J.I., Schwartz, S.Y., Protti, J.M., & Gonzalez, V. (2011), Persistent tremor within the northern Costa Rica seismogenic zone. *Geophysical Research Letters.* https://doi.org/10.1029/2010GL045586

Walter, J.I., Schwartz, S.Y., Protti, M., & Gonzalez, V. (2013), The synchronous occurrence of shallow tremor and very low frequency earthquakes offshore of the Nicoya Peninsula, Costa Rica. *Geophysical Research Letters*. https://doi.org/10.1002/grl.50213

Wech, A.G. (2016), Extending Alaska's plate boundary: Tectonic tremor generated by Yakutat subduction. *Geology*. https://doi.org/10.1130/G37817.1

Wech, A.G., Boese, C.M., Stern, T.A., & Townend, J. (2012), Tectonic tremor and deep slow slip on the Alpine Fault. *Geophysical Research Letters*. https://doi.org/10.1029/2012GL051751

Wech, A.G., & Creager, K.C. (2008), Automated detection and location of Cascadia tremor. *Geophysical Research Letters*. https://doi.org/10.1029/2008GL035458

Wessel, P., Smith, W.H.F., Scharroo, R., Luis, J., & Wobbe, F. (2013), Generic mapping tools: Improved version released. Eos (Washington. DC). https://doi.org/10.1002/2013EO450001

Wollin, C., Bohnhoff, M., Martínez-Garzón, P., Küperkoch, L., & Raub, C. (2018), A unified earthquake catalogue for the Sea of Marmara Region, Turkey, based on automatized phase picking and travel-time inversion: Seismotectonic implications. *Tectonophysics*. https://doi.org/10.1016/j.tecto.2018.05.020

Yabe, S., Ide, S., & Yoshioka, S. (2014), Along-strike variations in temperature and tectonic tremor activity along the hikurangi subduction zone, New Zealand. *Earth, Planets and Space*. https://doi.org/10.1186/s40623-014-0142-6

Yang, H., & Peng, Z. (2013), Lack of additional triggered tectonic tremor around the Simi Valley and the San Gabriel Mountain in southern California. *Bulletin of the Seismological Society of America*. https://doi.org/10.1785/0120130117

Zor, E., Özalaybey, S., & Gürbüz, C. (2006), The crustal structure of the eastern Marmara region, Turkey by teleseismic receiver functions. *Geophysical Journal International*.

https://doi.org/10.1111/j.1365-246X.2006.03042.x

Supporting References

Horstmann, T., Harrington, R. M., & Cochran, E. S. (2013), Semiautomated tremor detection using a combined cross-correlation and neural network approach. *Journal of Geophysical Research: Solid Earth*, 118(9), 4827-4846. https://doi.org/10.1002/jgrb.50345

Karabulut, H., Schmittbuhl, J., Özalaybey, S., Lengliné, O., Kömeç-Mutlu, A., Durand, V., Bouchon, M., Daniel, G., & Bouin, M.P. (2011), Evolution of the seismicity in the eastern Marmara Sea a decade before and after the 17 August 1999 Izmit earthquake. *Tectonophysics*. https://doi.org/10.1016/j.tecto.2011.07.009

Kassaras, I., Kapetanidis, V., & Karakonstantis, A. (2016), On the spatial distribution of seismicity and the 3D tectonic stress field in western Greece. *Physics and Chemistry of the Earth.* https://doi.org/10.1016/j.pce.2016.03.012

Journal of Geophysical Research Solid Earth

Supporting Information for

Does deep non-volcanic tremor occur in the central-eastern Mediterranean basin?

G. M., Bocchini[1], P., Martínez-Garzón[2], R. M., Harrington[1], and M., Bohnhoff[2-3],

[1]Faculty of Geosciences, Institute of Geology, Mineralogy, and Geophysics, Ruhr University Bochum, Bochum, Germany

[2]Helmholtz Centre Potsdam GFZ German Research Centre for Geosciences, Section 4.2 Geomechanics and Scientific Drilling

[3]Institute of Geological Sciences, Free University of Berlin, Berlin, Germany.

Corresponding author: Gian Maria and Bocchini (gian.bocchini@rub.de)

Contents of this file

Introduction

This supplements a detailed description of the cross-correlation envelop method used to search for ambient tremor during the occurrence of aseismic slip transients at the Hellenic Subduction Zone and in the eastern Sea of Marmara, and of the seismic network configuration in the two regions (Text S1). The two regions and the available seismic stations are visible in Figure S1. In Figure S2, we report an example of tectonic tremor detected by using the cross-correlation envelope method used in this study. We run the code, with the same settings we used for the eastern Sea of Marmara (Text S1), using land stations around the Cholame segment of the San Andreas Fault where tremor activity has been widely documented (see manuscript). In Figure S3, we show a burst of signals recorded by a station in Lipari (Eolian Volcanic Arc, Italy) potentially triggered by Love wave induced ground shaking from the 2011 Tohoku (Japan) earthquake. After careful inspection of the waveforms from one day before to one day after we conclude that signals are likely noise given their continuous occurrence over the inspected period when Signal-to-Noise-Ratio levels are lower. In Figure S4 we show a potentially triggered low frequency event at stations in Stromboli (Eolian Volcanic Arc, Italy) during the surface wave shaking of the 2015 Illapel (Chile) earthquake. We can not confirm the triggered nature of the signal because several similar low frequency events are visible before and after the ground shaking induced by the mainshock. Statistical tests comparing the number of events before and after the mainshock would be needed to support the triggered nature of the signal, but it is not in the scope of this study. In fact, the signal is very likely of volcanic origin given the 100 km depth of the plate interface beneath Stromboli. In Figure S5 we show a potential tremor-like signal observed at seismic stations on Crete (Greece) slightly before the arrival of Love waves from the 2015 Illapel (Chile) earthquake. The observation of the signal when PGV values are significantly lower than 0.01 cm/s suggest its spontaneous rather than triggered nature. No similar signals are observed in the day before and after its detection. Table S1 delineates the complete list of candidate mainshocks used for the analysis of triggered tremor.

Text S1.

We employ the envelope cross-correlation method (Ide, 2012, 2010) for the detection and hypocentral location of tremor signals. Raw daily traces are processed in Obspy as follows: (1) bandpass filtered between 2 and 8 Hz; (2) squared; (3) lowpass filtered below 0.1 Hz; (4) and resampled to 1 Hz. The procedure does not create waveform envelopes *sensu stricto* calculated with the Hilbert transform of original waves, but the difference is negligible and allows for faster processing. Envelope correlation is performed only on horizontal channels where tremor signals are expected to exhibit larger amplitudes. For the eastern Marmara Sea, where a shorter time period (~2 months) was investigated, we test varying half-overlapping windows (2, 3, 5 minutes), correlation thresholds (from 0.5 to 0.7) between stations located <100 km apart, and minimum number of horizontal components (from 5 to 8) at which the correlation threshold should be exceeded. When using shorter time windows (2-3 minutes), we required higher cross-correlation coefficients to be exceeded (0.7) at a higher number of channels (8) to limit the number of false detections. Conversely, when using longer time windows of 5 minutes we require lower cross-correlation coefficients to be exceeded (as low as 0.5) at a smaller number of channels (from 5 to 6). In case of the Hellenic Subduction Zone, where the two aseismic transient lasted about 1 year (~6 months each transient and ~4 months each SSE), we used half-overlapping windows of 5 minutes, and cross-correlation thresholds of 0.6 between stations located <100 km apart to be exceeded at a minimum number of 5 horizontal components.

To mitigate the unwanted effects of outliers, the code employs data outlier rejection algorithms. First, it performs a comparison of epicentral distances and travel times for a pair of stations to determine the initial epicenter, and then it associates the best hypocentral depth to it. In the first step, if the differential time between station pairs is larger than the difference in epicentral distance divided by the minimum S-wave velocity in the assumed structure by a certain threshold (i.e. 3 sec), the differential time data is rejected as an outlier. In the second step, if the error between the observed and calculated differential times for a pair of stations is more than three times larger than their standard deviation, the observed differential time data is rejected, and the hypocentral location is calculated again. The latter procedure is repeated until no differential time data is rejected. The envelope correlation method does not distinguish tremor from ordinary earthquakes, therefore we visually inspect all the detections to identify the nature of the signals. We refer the reader to Ide (2012) for further details on the method.

To allow for the best determination of hypocentral locations and enhance detectability of events, we use local S-wave velocity models. For the eastern Marmara Sea, we use the S-wave velocity model from Karabulut et al. (2011), while for the western segment of the Hellenic Subduction Zone, we use the S-wave velocity model from Kassaras et al. (2016).

We are aware of the limitations of applying such method in our cases of study where very dense station coverage is not available (Fig. 1S) and the intense background activity, especially true for the western segment of Hellenic Subduction Zone, could mask possible tremor signals. We therefore describe the network configuration in detail to make the reader aware of such possible limitations that mask small amplitude signals, such as tectonic tremor.

In the eastern Marmara Sea, to search for tremor activity possibly associated with the slow slip event starting on June 25, 2016 and lasting for about 50 days (Martínez-Garzón et al., 2019) we had an average number of 10 seismic stations available, including 3 boreholes, in the immediate proximity of the Çınarcık Fault (latitude from 40.5 to 41 and longitude from 28.5 to 30). The average interstation distance within the region is of ~20-25 km with most of the stations located to the south of the Çınarcık Fault, on the Armutlu Peninsula. In the broader area of the Sea of Marmara (latitude from 40.2 to 41.3 and longitude from 26.9 to 31) the maximum number of stations increases up to ~25 while the average interstation distance is ~100 km. We use seismic stations operated by the Kandilli Observatory and Earthquake Research Institute (KOERI, http://www.koeri.boun.edu.tr/new/en), from the Armutlu Network deployment (ARNET, Tunç et al., 2011), from the Disaster & Emergency Management Authority (AFAD) seismic network (https://deprem.afad.gov.tr/), and boreholes from the Geophysical borehole Observatory at the North Anatolian Fault (GONAF) deployment (Bohnhoff et al., 2017). We investigated the time period going from the 2nd of June 2016 to the 30th of July 2016.

To search for ambient tremor evidence during the two slow-slip events in 2014-2015 and 2018 along the western segment of the Hellenic Subduction Zone (Mouslopoulou et al., 2020), we used land stations of the Hellenic Unified Seismic Network operated by the National Observatory of Athens (http://bbnet.gein.noa.gr), the University of Patra (http://seismo.geology.upatras.gr/heliplots), the National and Kapodistrian University of Athens (http://dggsl.geol.uoa.gr/), and one additional station operated by the Technological Educational Institute of Crete (http://gaia.chania.teicrete.gr/uk/). During the 2014-2015 geodetic transient (09/24/2014-03/20/2015), we had available up to 13-14 land stations, deployed on Peloponnese, Zakynthos and Kefalonia (latitude from 36.4 to 38.2 and longitude from 19 to 23.2), with an average interstation distance of ~90-100 km. During the 2018 geodetic transient (05/14/2018-10/25/2018), the number of stations was slightly lower (up to 11-12) and therefore the average interstation distance slightly larger (~95-110 km).

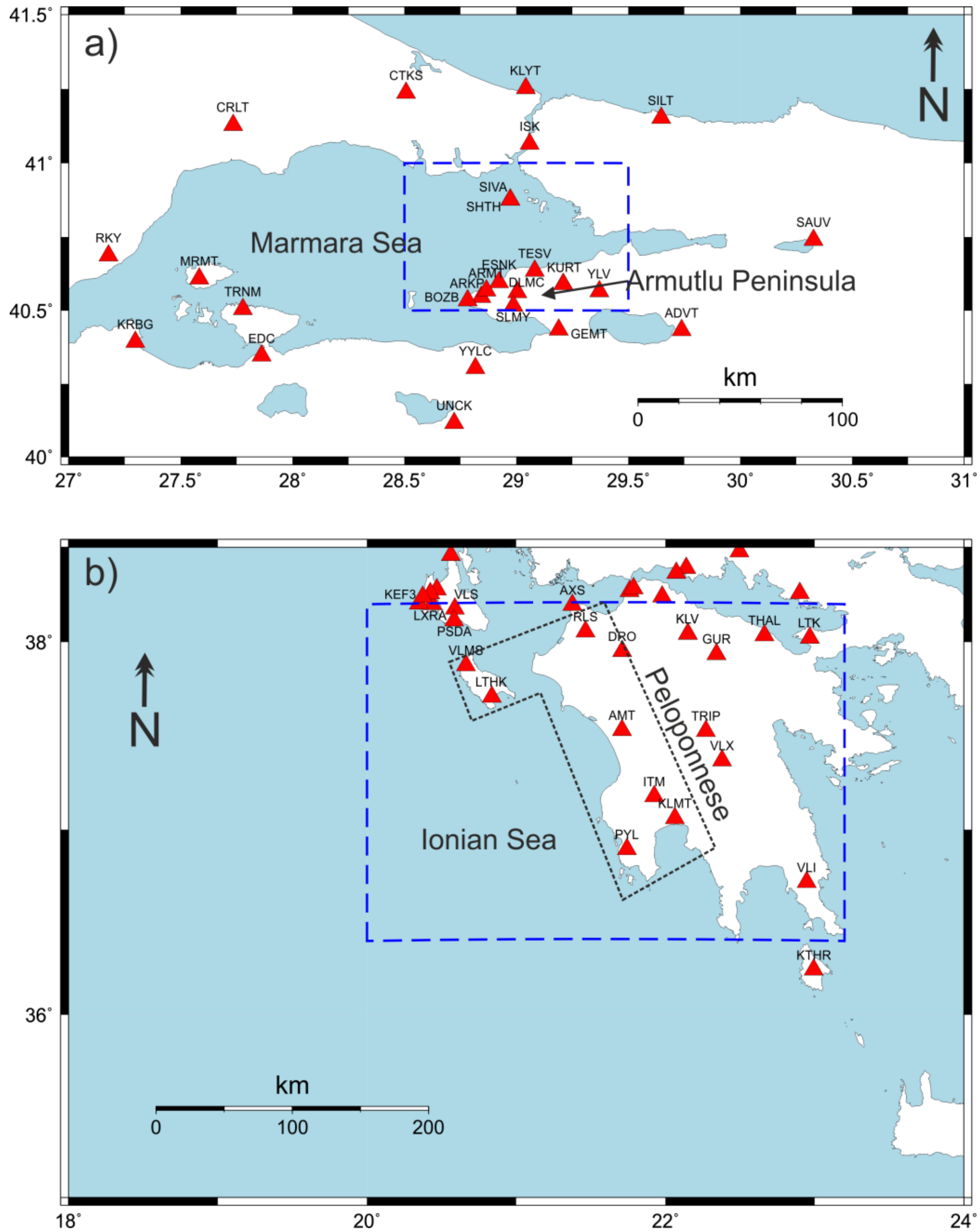

Figure S1. Maximum number of available seismic stations during the occurrence of the slow slip events in (a) the eastern Marmara Sea, and (b) along the western segment of the Hellenic Subduction Zone. The dashed blue boxes surround the closer seismic stations to the slow slip event sources and therefore the region where tectonic tremor would most likely be generated. In the eastern Marmara Sea (a) stations within the dashed blue box have an average interstation distance of 20-25 km, while along the western segment of the Hellenic Subduction Zone (b), stations within the dashed blue box have an interstation distance of 90-110 km. In subfigure b the dashed black line indicates the portion of the plate interface that slipped during the two slow slip events recorded by Mouslopoulou et al. (2020).

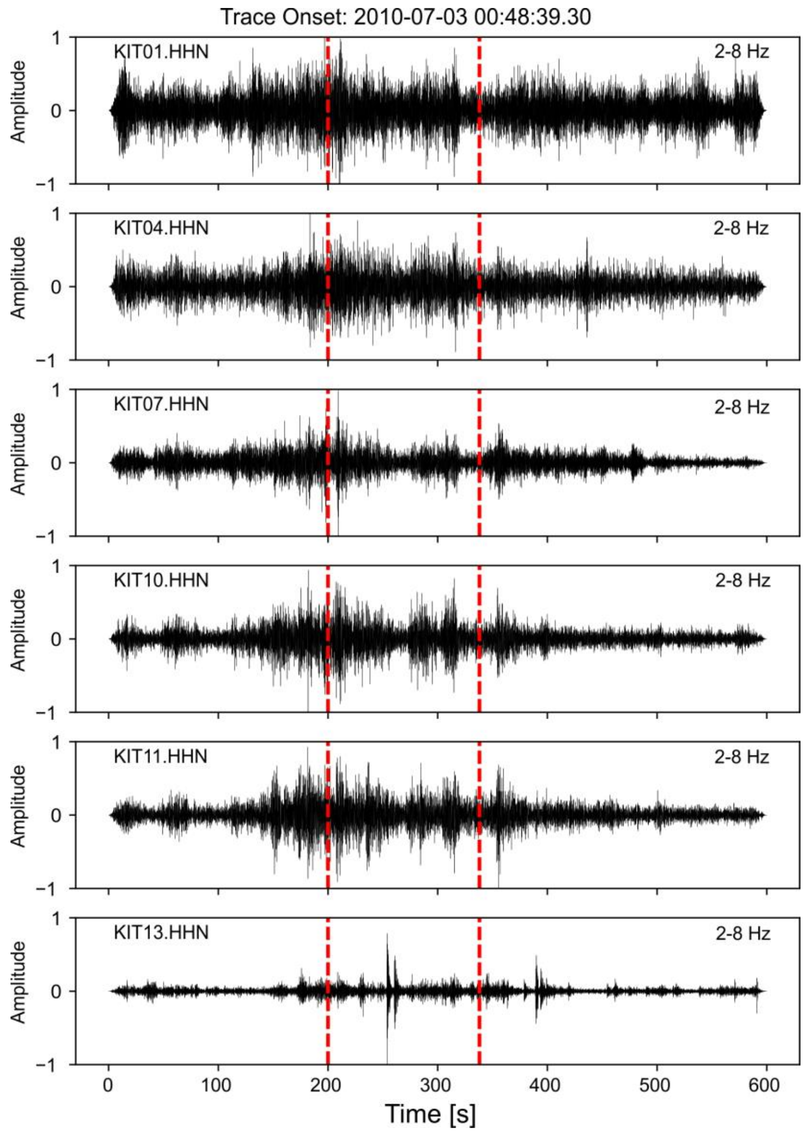

Figure S2. Example of tectonic tremor detected by using the cross-correlation method described in Text S1 and used in this study to detect tremor during documented slow slip events in the central-eastern Mediterranean basin. The signal is detected close to the Cholame segment of the San Andreas Fault, where the occurrence of tremor is widely documented (see manuscript). We used land stations from the Karlsruhe Broadband Array (Horstmann et al., 2013), half overlapping windows of 300 sec and cross-correlation (CC) coefficients of 0.5-0.6 to be exceed at a minimum of 6 components between 0.3 and 100 km apart. We used the same S-velocity model we used for the eastern Sea of Marmara (Text S1). When using a CC coefficient of 0.6 we obtain only the first detection while when lowering the CC coefficient to 0.5 we obtain both the detections shown in the figure. All traces are bandpass filtered between 2 and 8 Hz and time refers to the onset of the trace reported on top of the figure. The detected signal is also reported in the catalog of (Horstmann et al., 2013)

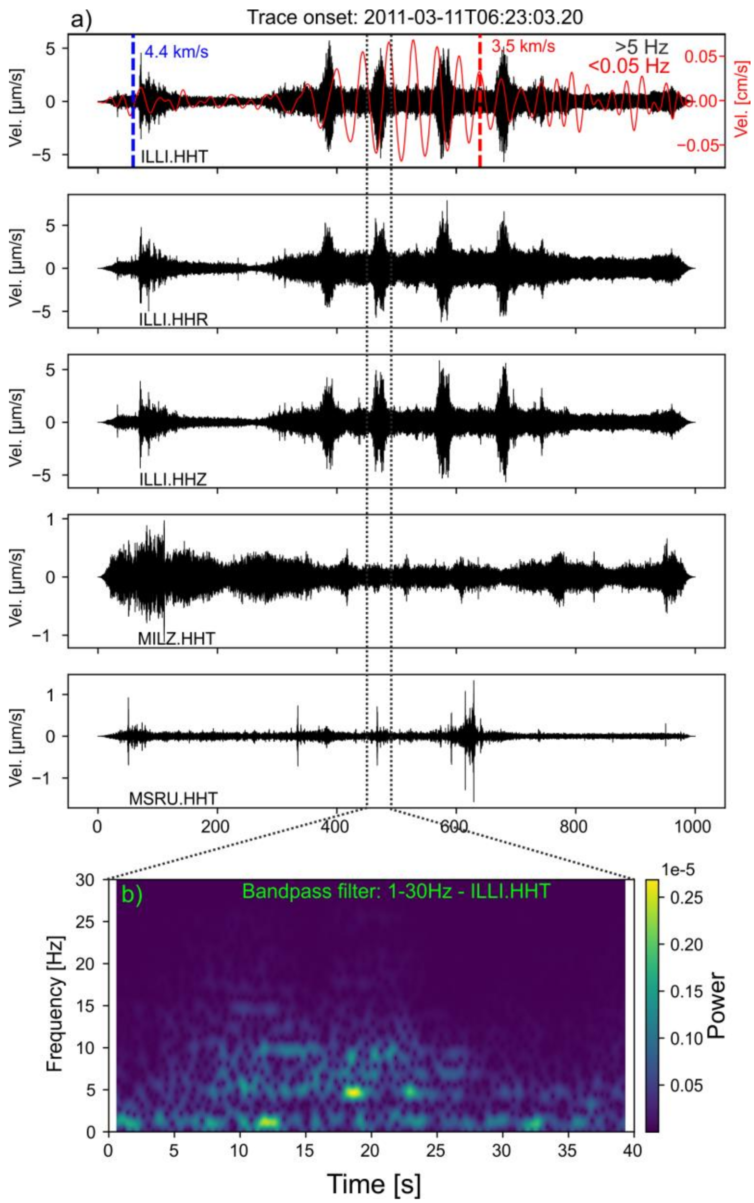

Figure S3. Possible low frequency signal detected at station ILLI (Lipari Island, Aeolian Volcanic Arc, Italy) during the passage of Love waves of the Mw 9.1 11-03-2011 Tohoku earthquake (Japan). The signal is interpreted as noise (see Section 4.1 manuscript). The topmost panel shows overlapping low frequency (<0.05 Hz, red) and high frequency waveforms (>5 Hz, black). (a) The signal is not visible at stations distant about 50 km from ILLI (e.g. MILZ, MSRU). (b) Spectrogram of one of the four bursts showing a frequency content below 10 Hz. The signal window shown in the spectrogram is indicated in the 2nd sub-figure from the top. Dotted blue and red lines in the top panel indicate the predicted arrival time of phases travelling at 4.4 km/s and 3.5 m/s, respectively, used to estimate the arrival time of Love and Rayleigh phases. Figure 2b of the manuscript indicates the station location. The dashed vertical line indicates the time window shown in the spectrogram.

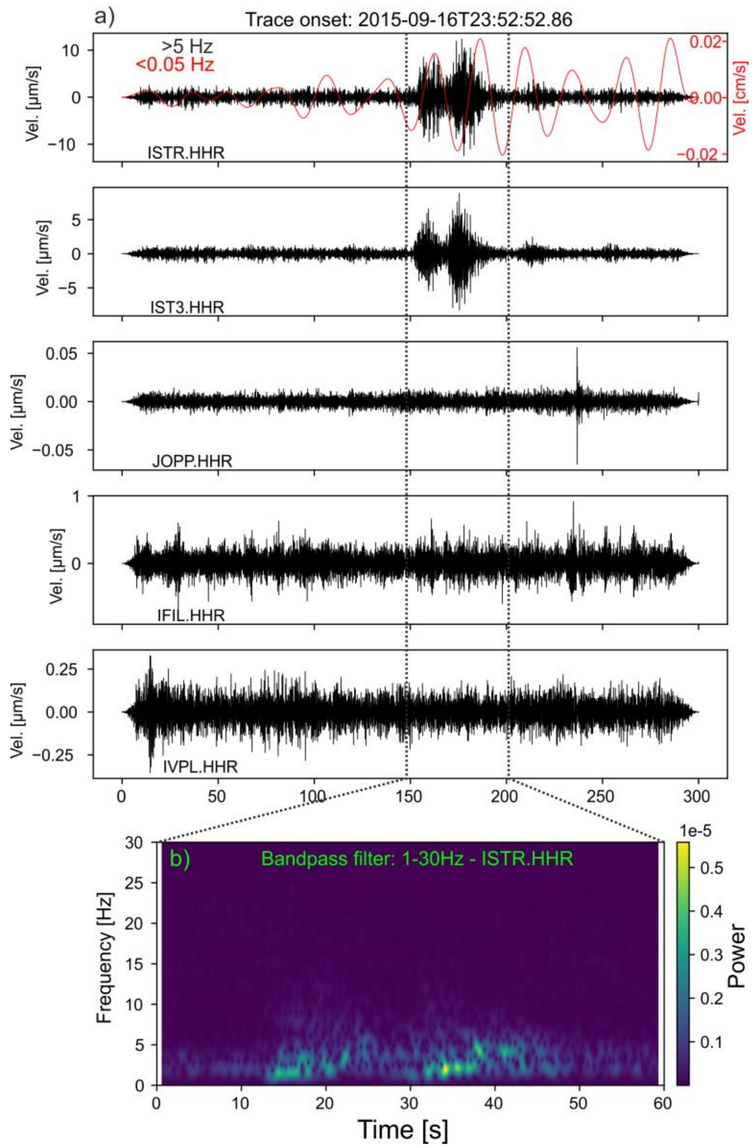

Figure S4. Possible low frequency earthquakes (LFEs) of volcanic origin detected at station ISTR and IST3 (Stromboli Island, Aeolian Volcanic Arc, Italy) during the passage of Rayleigh waves generated from the Mw 8.3 16-09-2015 Illapel earthquake (Chile). The interpretation of the detected signal as triggered event is not straightforward because numerous LFEs occur the day before and after the mainshock (see Section 4.1 manuscript). The top panel shows overlapping low frequency (<0.05 Hz, red) and high frequency waveforms (>5 Hz, black). (a) The signal is not visible at stations > 50 km from Stromboli (e.g. JOPP, IFIL, IVPL), confirming its local origin. (b) Spectrogram of one of the four bursts showing a frequency content below 5-8 Hz. The signal window shown in the spectrogram is indicated in the topmost panel. Figure 2b of the manuscript indicates the station location. The dashed vertical line indicates the time window shown in the spectrogram.

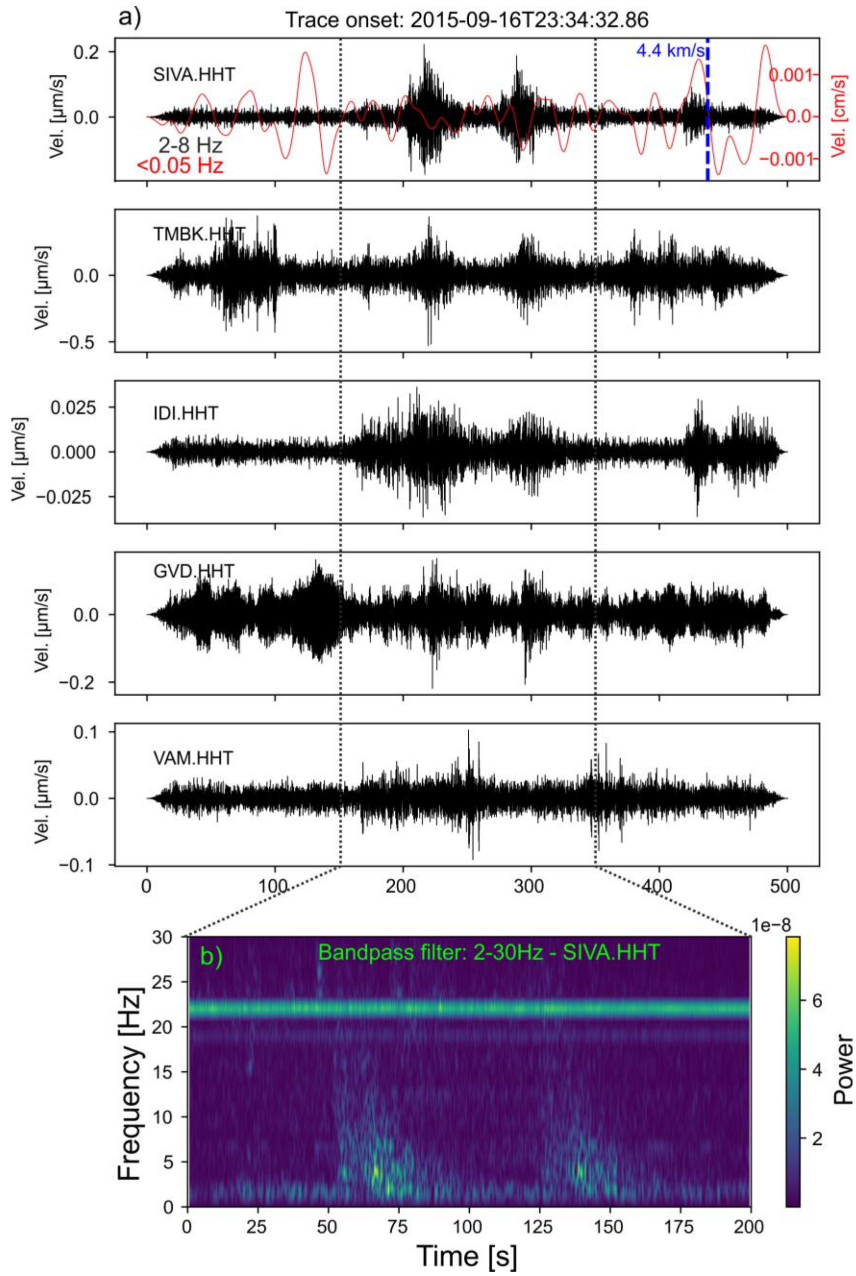

Figure S5. Possible low frequency signals detected at station on Crete before the passage of Love waves generated from the Mw 8.3, 16-09-2015 Illapel earthquake (Chile). The top panel shows overlapping low frequency (<0.05 Hz, red) and high frequency waveforms (2-8 Hz, black). (a) The signal is only visible at nearby stations supporting its local origin. (b) The spectrogram of the observed signal shows a frequency content below 8-10 Hz. The signal window shown in the spectrogram is indicated in the topmost panel. Figure 2c of the manuscript indicates the station location. Notice in the topmost panel the low peak ground velocities (20s period) at the time when the possible low frequency signal is detected. The dashed vertical line indicates the time window shown in the spectrogram.

ID	Date and Time	Fault type	Mw	Lat	Lon	Depth	Where is PGV exceeded	Epicentral Region
1	27/02/2010 06:34:13	T	8,8	-36,1485	-72,9327	28,1	a,b,c,d	Maule, Chile
2	06/04/2010 22:15:02	T	7,8	2,3601	97,1113	33,4	a,c,d	Sumatra, Indonesia
3	25/10/2010 14:42:22	T	7,8	-3,5248	100,104	20,0	-	Sumatra, Indonesia
4	11/03/2011 05:46:23	T	9,1	38,2963	142,498	19,7	a,b,c,d	Tohoku, Japan
5	23/10/2011 10:41:22	T	7,1	38,7294	43,4465	7,6	a,b,c,d	Turkey
6	11/04/2012 08:38:38	SS	8,6	2,2376	93,0144	26,3	a,b,c,d	Sumatra, Indonesia
7	11/04/2012 10:43:11	SS	8,2	0,7675	92,4284	21,6	a,b,c,d	Sumatra, Indonesia
8	11/08/2012 12:23:18	SS	6,5	38,4023	46,838	8,7	d	Armenia
9	28/10/2012 03:04:08	T	7,8	52,6777	-132,172	7,4	a,b,c	British Columbia, Canada
10	24/09/2013 11:29:48	SS	7,8	26,9109	65,5315	15,5	a,b,c,d	Pakistan
11	01/04/2014 23:46:47	T	8,1	-19,6193	-70,7877	17,1	a,b,c,d	Chile
12	24/05/2014 09:25:03	SS	6,9	40,2857	25,4032	28,3	b	Aegean Sea, Greece
13	13/02/2015 18:59:14	SS	7,1	52,5097	-32,0209	16,9	-	Reykjanes Ridge, Atlantic Ocean
14	25/04/2015 06:11:27	T	7,9	28,1302	84,7168	13,4	a	Nepal
15	16/09/2015 22:54:33	T	8,3	-31,5729	-71,6744	22,4	a,b,c,d	Illapel, Chile
16	07/12/2015 07:50:06	SS	7,2	38,2107	72,7797	22,0	c,d	Tajikistan
17	02/03/2016 12:49:48	SS	7,8	-4,9521	94,3299	24,0	a,b,c,d	Sumatra, Indonesia
18	16/04/2016 23:58:37	T	7,8	0,3819	-79,9218	20,6	-	Ecuador
19	30/10/2016 06:40:19	N	6,6	42,8547	13,0884	10,0	c,d	Amatrice, Italy
20	17/07/2017 23:34:14	SS	7,7	54,4715	168,815	11,0	a,b,d	Kamčatka, Russia
21	20/07/2017 22:31:11	N	6,6	36,9643	27,4332	10,2	b	Kos, Greece
22	12/11/2017 18:18:17	T	7,3	34,9052	45,9563	19,0	a,b,c,d	Iran
23	23/01/2018 09:31:43	T	7,9	56,0464	-149,073	25,0	a,b,c,d	Alaska
24	25/10/2018 22:54:53	SS	6,8	37,5148	20,5635	14,0	d	Zakynthos, Greece
25	24/01/2020 17:55:14	SS	6,7	38,3897	39,0883	10,0	a,b,c,d	Turkey
26	28/01/2020 19:10:25	SS	7,7	19,421	-78,7627	14,8	-	Cuba

Table S1. List of initially selected mainshocks to undergo visual inspection for triggered tremor evidence. PGV values are reported in Figure 3 of the manuscript. Focal mechanism solutions are retrieved from the United States Geological Service (USGS, https://earthquake.usgs.gov/) while M_w are from the International Seismological Centre (ISC) catalogue. Letters a, b, c, d in the 8th column indicate in which region the average calculated PGV for each event exceeded the 0.01 cm/s threshold. a) Kefalonia Transform Fault; b) Calabrian Subduction Zone; c) Hellenic Subduction Zone (Crete); d) North Anatolian Fault (eastern Marmara Sea)